Title: ***Transcription factors SlMYB41, SlMYB92 and SlWRKY71 regulate gene expression in the tomato exodermis***

Authors: Leonardo Jo*[1], Sara Buti*[1], Mariana A. S. Artur*[1,2], Rianne M.C. Kluck*[1], Alex Cantó-Pastor[3,4], Siobhán M. Brady[3,5], Kaisa Kajala[1]

Names and addresses of the institutions:

[1] Experimental & Computational Plant Development, Institute of Environmental Biology, Utrecht University, Utrecht, the Netherlands

[2]Laboratory of Plant Physiology, Wageningen Seed Science Centre, Wageningen University and Research, Wageningen 6708PB, the Netherlands

[3] Department of Plant Biology and Genome Center, University of California, Davis, Davis, CA, USA

[4]Present address: Department of Molecular, Cellular and Developmental Biology, Faculty of Arts and Sciences, Yale University, New Haven, CT, USA

[5]Howard Hughes Medical Institute, University of California, Davis, Davis, CA USA

* These authors contributed equally.

Email address for each author:

l.jo@uu.nl
s.buti@uu.nl
mariana.silvaartur@wur.nl
r.m.c.kluck@uu.nl
alex.cantopastor@yale.edu
sbrady@ucdavis.edu
k.kajala@uu.nl corresponding author

Date of submission: 24th October 2024

Word count: 5828

Article includes 4 figures, 5 supplementary figures, 7 supplementary tables and 2 datasets.

Running title: MYB41, MYB92 and WRKY71 regulate tomato exodermis

Highlight

MYB and WRKY transcription factors collaboratively regulate suberin biosynthesis in the tomato root exodermis. Antagonistic interactions may fine-tune suberization or act as a break to stop overaccumulation.

Abstract

Root barrier cell types, like the endodermis and exodermis, are crucial for plant acclimation to environmental stresses. Deposition of suberin, a hydrophobic polymer, in these cell layers restricts the movement of molecules and plays a vital role in stress responses. This study investigates the role of SlMYB41, SlMYB92 and SlWRKY71 transcription factors (TFs) in regulating suberin biosynthesis in the tomato (*Solanum lycopersicum*) root exodermis by genetic perturbation. Genetic perturbation of these TFs altered exodermal suberin deposition patterns, indicating the SlMYBs as positive and SlWRKY71 negative regulators of suberization. RNA sequencing revealed a significant overlap between differentially expressed genes regulated by these TFs, suggesting a shared regulatory network. Gene set enrichment analyses highlighted their role in lipid and suberin biosynthesis as well as overrepresentation of exodermis-enriched transcripts. Furthermore, transactivation assays demonstrated that these two MYBs promote the expression of suberin-related genes, while SlWRKY71 represses them. These results indicate a complex antagonistic relationship, advancing our understanding of the regulatory mechanisms controlling exodermis suberization in tomato roots.

Keywords

Suberin, MYBs, WRKYs, exodermis, trans-activation assays.

Abbreviations

ABCG	ATP-binding cassette transporters of the subfamily G
ASFT	Aliphatic suberin feruloyl transferase
BF	Basic fuchsin
CW	Calcofluor white
CYP	CYTOCHROME P450
DEG	Differentially Expressed Gene
FA	Fatty Acid
FY	Fluorol yellow
GELP	GDSL-type Esterase/Lipase Protein
GO	Gene ontology
GPAT	Glycerol-3-phosphate acyltransferase
GRN	Gene regulatory network
KCS	Ketoacyl-CoA synthase
LACS	Laccase
LTP	Lipid transfer protein
ko	knock out
MDS	Multidimensional scaling

MYB	Myeoloblastosis
OX	Overexpressor
TF	Transcription factor
VLCFA	Very-long-chain fatty acid

Introduction

Root barrier cell types emerged as an evolutionary innovation that allows plants to interact and acclimate to their local environment. The endodermis and exodermis are known as two very important root barrier cell types that control the movement of molecules and solutes into the roots and their exudation into the plant's environment (Liu and Kreszies, 2023). The endodermis is the innermost ground tissue cell layer localized next to the pericycle, and it is found in all vascular plants. It is characterized by the deposition of two hydrophobic barriers, the lignified Casparian strip and the suberin lamellae, which restrict the diffusion of molecules between the root vasculature and the surrounding environment (Robbins *et al.*, 2014; Barberon *et al.*, 2016; Doblas *et al.*, 2017). The Casparian strip is deposited in the anticlinal walls of endodermis cells and provides a barrier for the apoplastic transport of ions and solutes, while suberin lamellae are deposited outside the plasma membrane just below the primary cell wall and prevent diffusion through the plasma membrane (Robbins *et al.*, 2014; Shukla and Barberon, 2021). Because of the deposition of these hydrophobic barriers, the movement of molecules such as ions, hormones, nutrients and immunosignals are constricted to pass through the endodermis cytoplasm. Therefore, the endodermis cell layer has been proposed to act as signaling hub for root cell communication (Miyashima and Nakajima, 2011; Robbins *et al.*, 2014; Salas-González *et al.*, 2021; Xu *et al.*, 2022*b*; Verbon *et al.*, 2023). The exodermis is the outermost cortex layer found beneath the epidermis. Similar to the endodermis, exodermal barriers are usually composed of lignin and suberin (Barberon, 2017; Liu and Kreszies, 2023). Due to the deposition of these hydrophobic polymers, the exodermis also is an important barrier cell type in the root system, and its appearance was also an important step on plant adaptation to dry land (Ranathunge *et al.*, 2011; Artur and Kajala, 2021; Liu and Kreszies, 2023). Exodermis suberization contributes to the plant drought response (Cantó-Pastor *et al.*, 2024), and can act as a radial oxygen loss (ROL) barrier during flooding (Ejiri and Shiono, 2019). However, different from the endodermis, the exodermis is only found in the roots of some plant species (Artur and Kajala, 2021), particularly not in the model species *Arabidopsis thaliana*. For this reason, the endodermis has been the best-characterized barrier cell type in roots.

The suberization of barrier cell types is plastic under a wide range of abiotic and biotic cues such as osmotic, salinity, drought, nutrients, pathogens and the soil microbiome (Ranathunge *et al.*, 2011; Barberon *et al.*, 2016; Kreszies *et al.*, 2020; Feng *et al.*, 2022; Lu *et al.*, 2022; Su *et al.*, 2023; Kawa *et al.*, 2024). Recent genetic and molecular research has identified major players of suberin biosynthesis and polymerization in response to developmental and environmental cues.

MYB (Myeloblastosis) transcription factors (TFs) have been identified as major coordinators of the expression of suberin biosynthesis genes in the Arabidopsis root endodermis (Shukla *et al.*, 2021; Xu *et al.*, 2022*b*) and seed coat (Gou *et al.*, 2017). *AtMYB41* was found to induce the ectopic expression of suberin biosynthesis genes and deposition of suberin-like lamellae in multiple plant species and cell types (Kosma *et al.*, 2014). *AtMYB39* and *AtMYB92* have also been shown to enhance suberin lamellae deposition when heterologously expressed in *Nicotiana benthamiana* leaves (Cohen *et al.*, 2020; To *et al.*, 2020). MYBs have also been shown to form multiple transcriptional sub-regulatory networks to regulate suberization of the Arabidopsis endodermis (Xu *et al.*, 2022*b*). For example, Shukla *et al.*, (2021) identified the requirement of four MYB TFs (*AtMYB41*, *AtMYB53*, *AtMYB92* and *AtMYB93*) for Arabidopsis root endodermis suberization. MYBs have also recently been shown to be involved with regulation of suberin deposition in other plant species and organs, for example in rice roots (Huang *et al.*,

2024), cork oak (Capote *et al.*, 2018); sugar cane (Figueiredo *et al.*, 2020); kiwi fruits (Wei *et al.*, 2020*a*,*b*; Han *et al.*, 2022); apple fruit skins (Legay *et al.*, 2016; Xu *et al.*, 2022*a*); and in grapevine roots in response to drought (Zhang *et al.*, 2020). Furthermore, chemical composition and transcriptome analyses of tomato and russet apple fruit surfaces showed a conserved gene expression signature for suberin polymer assembly, and that homologs of *AtMYB107* and *AtMYB9* regulate suberin deposition developmentally in fruit surfaces and Arabidopsis seeds (Lashbrooke *et al.*, 2016).

Together with MYBs, WRKY TFs (named after their conserved N-terminal WRKYGQK motif) are emerging as potentially important regulators of suberin biosynthesis in Arabidopsis root endodermis. Arabidopsis *AtWRKY33* and *AtWRKY9* have been shown to be involved with suberization of root endodermis, conferring salt stress tolerance (Krishnamurthy *et al.*, 2020). Still, little is known about the participation of WRKY TFs in MYB-centered gene regulatory modules regulating suberin biosynthesis in the Arabidopsis endodermis and other plant species and cell types.

Although there is increasing information about the regulation of suberin biosynthesis in different plant organs as well as the control of endodermis suberization and its physiological relevance, little is known about the molecular mechanisms controlling exodermis suberization, despite its importance for plant physiology and root plasticity. This is mainly due to the absence of an exodermis in Arabidopsis roots (Liu and Kreszies, 2023). Shiono *et al.* (2014) investigated gene expression during the formation of the rice exodermal radial oxygen loss (ROL) barrier and identified several TFs, including MYBs and WRKYs, as potential regulators of the suberin biosynthesis genes in rice exodermis. More recently, Kajala *et al.* (2021) identified exodermis-enriched gene expression patterns in tomato roots (*Solanum lycopersicum*). For example, a WRKY TF (encoded by *Solyc02g071130.3.1*) and a MYB TF (SlMYB41 encoded by *Solyc02g079280.3.1*) were identified as exodermis-enriched (Kajala *et al.*, 2021). Reynoso *et al.* (2022) found that the plastic response of rice exodermis suberization and nutrient homeostasis in response to water deficit and rewatering might involve the interplay between MYBs and WRKYs in rice. Specifically, they identified a water-deficit-promoted suberin regulatory network gene promoters enriched in MYB and NAC TF binding sites (TFBSs). Conversely, they found that gene promoters related to iron homeostasis were enriched in basic helix-loop-helix (bHLH) and WRKY TFBSs and strongly downregulated during water deficit. Given that iron deficiency delays suberization in the endodermis (Barberon *et al.*, 2016), the MYBs and WRKYs may modulate the opposing dynamics of suberization and nutrient uptake in the rice exodermis.

The expression of tomato *WRKY Solyc02g071130.3.1* (here referred to as *SlWRKY71* according to homology to Arabidopsis *AtWRKY71* (Karkute *et al.*, 2018; Wang *et al.*, 2020*b*; Kumar *et al.*, 2023) has also been shown to change in response to drought stress in leaves (Karkute *et al.*, 2018), and in response to jasmonate and aluminum treatments in roots (Wang *et al.*, 2020*b*), which suggest a role in stress-responsive tomato environmental plasticity. Furthermore, recent research has shown that SlWRKY71 works as an inhibitor of gene expression to negatively regulate tomato fruit ripening (Sun *et al.*, 2023).

Recently, a set of MYB TFs (SlMYB41, SlMYB92, encoded by *Solyc05g051550.2.1,* and SlMYB63 encoded by *Solyc10g005550.3.1*) were shown to be necessary for suberin deposition of the tomato root exodermis, and the suberization of the exodermis contributing to the tomato drought response (Cantó-Pastor *et al.*, 2024). Whether MYBs and WRKYs act together to form a

regulatory module to control the expression of suberin biosynthesis genes in tomato root exodermis is yet to be explored.

To address this question, we investigated if SlMYB41, SlMYB92 and SlWRKY71 control the expression of suberin biosynthesis genes using overexpression (OX) and CRISPR-Cas9 knock-out (ko) mutants in tomato hairy root lines (Ron *et al.*, 2014). As previously reported (Cantó-Pastor *et al.*, 2024), we observed a reduction in suberin in *Slmyb41*-ko and *Slmyb92*-ko lines, while their overexpression did not alter the observed patterns. In contrast, we found that the exodermis suberin deposition was reduced in *SlWRKY71*-OX. We performed RNA-seq analysis on root tips from overexpression and knockout lines to identify genes regulated by SlMYB92, SlMYB41, and SlWRKY71. Knockout of these TFs significantly impacted the root tip transcriptome, with SlMYB92 and SlMYB41 showing overlapping gene regulation, particularly in lipid biosynthesis and oxidative stress pathways. Our transcriptome findings also suggested that SlMYB92 and SlMYB41 act as positive regulators, while SlWRKY71 serves as a repressor of suberin biosynthesis genes in the tomato root exodermis. Transactivation assays further confirmed that SlWRKY71 antagonizes the promoter activation by SlMYBs. Together, our findings highlight an interplay between these three TFs to fine-tune the expression of suberin biosynthesis gene in the tomato root exodermis.

Methods

Phylogenetic tree construction

We retrieved the AGI locus codes and nomenclature of Arabidopsis MYBs with described functions associated with suberization (Kosma *et al.*, 2014; Du *et al.*, 2015; Lashbrooke *et al.*, 2016; Gou *et al.*, 2017; Cohen *et al.*, 2020; Shukla *et al.*, 2021; Xu *et al.*, 2022*b*) from Dubos *et al.* (2010). For WRKYs, we retrieved AGI codes and nomenclature of Arabidopsis WRKY family members described by Eulgem *et al.* (2000) and Wu (2005) and we searched in the literature for the ones with described functions associated with suberization in multiple plant species (Supplementary Table S1). Using the gene identifiers we queried the primary protein sequences of MYBs and WRKYs in Phytozome 13 (https://phytozome-next.jgi.doe.gov/) using sequences from *Arabidopsis thaliana* genome TAIR10 (Goodstein *et al.*, 2012). For each TF family, we performed multiple sequence alignment using MAFFT online server (https://mafft.cbrc.jp/alignment/server/) using the standard automated method with the L-INS-i model. We used IQ-TREE webserver (http://iqtree.cibiv.univie.ac.at/) to infer a Maximum Likelihood tree with 1,000 bootstraps, and we edited the phylogenetic tree using iTOL (Letunic and Bork, 2016).

DNA constructs for gene editing and overexpression

We performed transcriptional reporter construct cloning and imaging as described in Kajala *et al.* (2021) and tomato CRISPR-Cas9 construct cloning, mutant line generation, and analyses according to Cantó-Pastor *et al.* (2024). We generated the overexpression lines by retrieving the coding sequence (CDS) of *SlMYB41* (*Solyc02g079280*), *SlMYB92* (*Solyc05g051550.2.1*) and *SlWRKY71* (*Solyc02g071130.3.1*) from the Sol Genomics database (https://solgenomics.net; ITAG3.2). We extracted RNA and synthesized cDNA from tomato (cultivar M82) as described by

210 Kajala *et al.* (2021). We amplified the CDS without the stop codon using primers listed in
211 Supplementary Table S2, purified the PCR products from the agarose gel using QIAquick Gel
212 Extraction kit and introduced the cleaned fragments into the pENTR/D-TOPO vector (Invitrogen)
213 following manufacturer's instructions. The previously described *35S* promoter (Ron *et al.*, 2014)
214 was cloned into the pENTR5'/TOPO (Invitrogen). We synthesized 3xFLAG oligodimer using the
215 primers listed in Supplementary Table S2 and introduced it into the pENTR/D-TOPO vectors
216 containing the CDSs to generate CDS-3xFLAG constructs using restriction site-based cloning.
217 To generate the final *35S*::CDS-3xFLAG binary vectors, we recombined the promoters and CDS-
218 3xFLAG fusions into the Multisite Gateway vector pK7m24GW
219 (https://gateway.psb.ugent.be/search) using LR Clonase II Enzyme mix (Invitrogen). All
220 constructs generated were confirmed by Sanger sequencing.

221 For the knock-down constructs of *SlWRKY71*, target guide-RNAs were generated using
222 the CRISPR-P (http://crispr.hzau.edu.cn/CRISPR2/) and CHOPCHOP
223 (https://chopchop.cbu.uib.no/) web-tools. Their specificity was accessed by blasting the core
224 sequence of the guide-RNA into the tomato ITAG4.0 genome version in phytozome
225 (https://phytozome-next.jgi.doe.gov/). Oligos for two guide-RNAs per target (Supplementary
226 Table S3) was synthesized and cloned into pMR217 and 218 vectors, and assembled with
227 Gateway into binary vector pMR290 as described earlier by Cantó-Pastor *et al.* (2024) (based on
228 Fauser *et al.*, 2014; Bari *et al.*, 2019). The final CRISPR constructs were then introduced to *R.*
229 *rhizogenes* (strain ATCC15834) and used for the subsequent hairy-root transformation steps.

230

231 ***Hairy root cultures and tomato transformation***

232 Hairy root cultures were generated following the protocols in Ron *et al.* (2014) as follows. To
233 generate competent *Rhizobium rhizogenes* (strain ATCC15834) cells, they were grown in MG/L
234 media (Ron *et al.*, 2014) at 28-29°C for 24-30 hours to a final optical density (OD_{600}) of 0.5-0.7. We
235 cooled the cells on ice for 15 minutes, spun at 500 rpm for 10 min and then resuspended them
236 in 0.01x of the culture volume of 10% glycerol. The aliquots were then immediately frozen in liquid
237 nitrogen and stored at -80°C until use. For transformation, we incubated *R. rhizogenes* aliquots
238 on ice with 1 µL of the desired plasmid DNA construct prior to electroporation. Then, we
239 immediately transferred cells to 1 mL of MG/L media and shaken at 28-29°C for 3 hours. We then
240 plated the whole aliquot on MG/L media with agar containing the appropriate antibiotics and
241 incubated for 3 days at 28-29°C.

242 To generate tomato hairy root cultures, we took the following steps: tomato seeds
243 (*Solanum lycopersicum* cv. M82, LA3475) were sterilized with 70% ethanol for 10 minutes, rinsed
244 with sterile MQ water, soaked in 50% commercial bleach for 10 minutes and rinsed three times
245 with sterile MQ water. We plated the seeds on MS media supplemented with 1% sucrose and
246 incubated under 16 h light : 8 h dark for 7-10 days. We cut the expanded cotyledons in sterile
247 conditions with a scalpel and immediately immersed in the desired *R. rhizogenes* suspension for
248 20 minutes, blotted on sterile Whatman filter paper and transferred to MS plates supplemented
249 with 3% sucrose without antibiotics for 3 days at 22-25°C in dark. After three days, we transferred
250 the explants bottom-side up to MS media supplemented with 3% sucrose, 200 mg/L cefotaxime
251 and the desired antibiotics for transformant selection and incubated at 22-25°C until roots
252 started to emerge. We transferred roots of about 1 cm length on the same media, and we
253 maintained the cultures by transferring 3-4 cm root segments onto fresh plates every 2-3 weeks.
254 After two rounds of culturing hairy roots, we placed them onto media without antibiotics.

255 We validated the hairy root cultures for successful gene editing events and protein
256 overexpression. To identify the deletions in the target genes, we amplified the genomic fragment
257 of *SlWRKY71,* and we identified the deleted region through Sanger sequencing (Supplementary
258 Figure S1). We validated the correct protein expression of the hairy root lines overexpressing
259 SlMYB41, SlMYB92 and SlWRKY71 through a Western blot experiment. After extracting total
260 protein lysates from the hairy root samples, we boiled the lysates for 1 min at 96°C and we loaded
261 them on a 4% to 15% mini-PROTEAN TGX stain-free protein gels (Bio-Rad). We transferred the
262 proteins onto a polyvinylidene difluoride (PVD) membrane using a Bio-Rad transblot turbo and
263 we blocked the blots with 5% (w/v) milk powder (Elk) in Tris-buffered saline (TBS) buffer. We
264 detected the proteins using the monoclonal antibody ANTI-FLAG M2 (Sigma no. F1804, 1:1000 in
265 0.5% [w/v] Elk TBS). We used the goat anti-mouse IgG conjugated with horseradish peroxidase
266 as secondary antibody (Cell Signaling Technology no. 7076, 1:2500 in 0.5% [w/v] Elk TBS plus
267 Tween 20 0.1% [v/v]). The labeled proteins were visualized using a 50/50 mix of
268 chemiluminescence substrates (cat no. 34096, Thermo Fisher Scientific) on a ChemiDoc
269 Imaging system (Bio-Rad).

270

271 ***Expression maps***

272 We created the spatial expression profiles of *SlMYB41*, *SlMYB92* and *SlWRKY71* using the R
273 package ggPlantmap (Jo and Kajala, 2024). The expression data used for plots was obtained from
274 the tomato translatome dataset from Kajala *et al.* (2021). Data plotted is from TRAP marker lines
275 driven by following promoters: epidermis *AtWER*, exodermis *SlPEP*, inner cortex *AtPEP*,
276 endodermis *SlSCR*, xylem *AtS18*, phloem *AtS32*.

277

278 ***Suberin & lignin histochemistry and imaging***

279 We prepared root cross sections of hairy roots subcultures of the control (empty vector),
280 *35S::MYB41-3xFLAG* (*SlMYB41*-OX), *35S::MYB92-3xFLAG* (*SlMYB92*-OX), *35S::WRKY71-3xFLAG*
281 (*SlWRKY71*-OX), *Slmyb41*-ko, *Slmyb92*-ko, *Slwrky71*-ko(4), and *Slwrky71*-ko(5) that had grown
282 for 3 weeks at 20°C. We selected newly emerged roots from the previous subculture. Of those
283 selected roots, we harvested 2-cm sections located in regions with newly emerging lateral roots.
284 After harvest, we fixed the roots by vacuum infiltrating with 4% paraformaldehyde (Thermo
285 Scientific) for 1 h. After that, we placed the roots in ClearSee (Ursache *et al.*, 2018) for a minimum
286 of three days. We embedded the cleared and harvested pieces in 3.5% agarose (Fisher Scientific)
287 and prepared 250 µm thick sections using the VT 1000 S vibratome (Leica). To visualize suberin,
288 we incubated the cross sections on a shaker in dark for 20 min in Fluorol Yellow 088 (Chem Cruz,
289 Santa Cruz Biotechnology Inc.) (FY; 0.01% w/v in 96% ethanol, first dissolved in 1 ml DMSO (0.5%
290 (w/v)). After that, we counterstained the sections using aniline blue (Sigma Aldrich) (0.5% w/v,
291 dissolved in water) and placed them on a shaker in dark for 20 min at room temperature. We
292 rinsed the sections with MQ water until the excess aniline blue was completely washed off and
293 kept them in 50% glycerol until imaging. To visualize lignin, we stained the cross-sections with
294 Basic Fuchsin (BF; 0,2% w/v, dissolved in ClearSee (Ursache *et al.*, 2018)) and Calcofluor White
295 (CW; 0,1 % w/v, dissolved in ClearSee). We first stained the sections with BF on a shaker in the
296 dark for 20 min at room temperature. The BF was rinsed off with four washes of ClearSee of 15
297 min each. Afterwards, we stained the sections with CW and the excess was washed off with
298 ClearSee. After this final wash of 30 min, we kept the stained sections in 50% glycerol until

299 imaging. We imaged all stained samples on the same day using the Zeiss Airyscan LSM 880.
300 Samples stained with FY were imaged using 488 nm excitation and 500-550 nm detection range.
301 Samples stained with BF & CW were imaged using an excitation range of 561 nm and detection
302 range of 600-650 nm for BF, and using excitation range of 405 nm and a detection range of 425–
303 475 nm for CW.

304

305 ***RNAseq tissue harvest, library preparation and sequencing***

306 To collect the material for RNAseq, we subcultured the hairy roots of lines of the control (empty
307 vector), *35S::MYB41-3xFLAG* (*SlMYB41*-OX), *35S::MYB92-3xFLAG* (*SlMYB92*-OX), *35S::WRKY71-*
308 *3xFLAG* (*SlWRKY71*-OX), *Slmyb41*-ko, *Slmyb92*-ko, *Slwrky71*-ko(4), and *Slwrky71*-ko(5) on sterile
309 square Petri dishes (120x120x17 mm, Greiner Bio One) on MS medium (Duchefa Biochemie)
310 supplemented with 3% sucrose, 200 mg/L cefotaxime sodium (Duchefa Biochemie), 1% BD
311 Difco agar (Fisher Scientific), 0.5 g/L MES hydrate (Thermo Fisher Scientific) and grew them at
312 25°C in the dark. After 9 days of growth, we collected the first cm of 10 root tips for each of the
313 three biological replicates per line and snap-froze them in liquid nitrogen. The samples were
314 collected in 2-ml tubes containing ceramic beads and ground using a tissuelyser (Retsch
315 MM300). The mRNA extraction and library preparation were performed according to the non-
316 strand specific random primer-primed RNAseq library protocol of Townsley *et al.* (2015). The
317 libraries were pair-end sequenced (50 bp) at Utrecht Sequencing Facility (Utrecht, The
318 Netherlands) using Illumina NextSeq2000.

319

320 ***RNA-seq data processing***

321 We quality trimmed paired-end reads using Trim Galore (version 0.6.6) (Krueger, 2015) using
322 default settings. After trimming, we pseudo-aligned the paired reads to the tomato reference
323 transcriptome version ITAG4.1 (Sol Genomics, https://solgenomics.net) using Kallisto (version
324 0.46.2) (Bray *et al.*, 2016) with the following parameters: -b 100. Pseudo-counts were then used
325 for differential expression analysis. All scripts used for the trimming and alignment can be found
326 in https://github.com/leonardojo/tomato-TF-exodermis-2024.

327

328 ***Differential expression analysis***

329 We identified differentially expressed genes (DEGs) using the R package limma (Ritchie *et al.*,
330 2015) according to Kajala *et al.* (2021, https://github.com/leonardojo/tomato-TF-exodermis-
331 2024). We set the threshold of adjusted P value < 0.05 for DEG identification. To obtain the DEGs,
332 we compared each mutant and overexpressor to the empty vector control hairy roots
333 (Supplementary Dataset S1). To identify candidate genes for transactivation assays, we
334 compiled an overview file (Supplementary Dataset S2) where we cross-referenced our DEGs with
335 exodermis-enriched transcripts (Kajala *et al.*, 2021) and a suberin module from tomato single
336 cell data (Cantó-Pastor *et al.*, 2024). We selected genes that were exodermis-enriched, good
337 candidates for suberin barrier formation, or DEGs in our data.

338

339 ***Gene ontology (GO) enrichment analysis***

340 We tested our DEG lists for GO term enrichment using the R package goseq (Young *et al.*, 2010).
341 GO functional annotation was extracted for ITAG4.0 from Phytozome 13 (https://phytozome-
342 next.jgi.doe.gov/). A q-value threshold of 0.05 was used to determine the enriched GO categories
343 in each DEG list.

344

345 ***Identification of tomato suberin biosynthesis genes***

346 To define the list of fatty-acid and suberin biosynthesis genes in tomato, we used the Tomato
347 Plant Metabolic Network database, TOMATOCYC 4.0
348 (https://plantcyc.org/databases/tomatocyc/4.0), and identified the tomato genes associated
349 with the following pathways and reactions: very long chain fatty acid biosynthesis I, very long
350 chain fatty acid biosynthesis II, suberin monomer biosynthesis and esterified suberin
351 biosynthesis.

352

353 ***DNA constructs for trans-activation assay: Promoters***

354 We extracted tomato genomic DNA from leaves of *Solanum lycopersicum* cultivar M82 and used
355 it as template. We used PCRBIO HiFi Polymerase (PCR Biosystems Ltd.) to amplify the promoter
356 regions of the genes listed in Supplementary Table S4 using the primers listed in Supplementary
357 Table S5. The PCR products were gel-purified using the kit NucleoSpin Gel and PCR Clean-up
358 (MACHEREY-NAGEL). We cloned all the promoters, except for *Solyc02g071130.3.1*, directly into
359 the destination vector pDLUC15 (Jo *et al.*, 2020) using the NEBuilder® HiFi DNA Assembly Cloning
360 Kit (NEB, England) after digesting it with the enzyme FastDigest *Hind*III (Thermo Fisher Scientific).
361 Instead, we cloned the promoter sequence of *Solyc02g071130.3.1* first into the Gateway vector
362 pDONR207 (Thermo Fisher Scientific) using the Gateway BP clonase II enzyme mix (Thermo
363 Fisher Scientific) and subsequently into the Gateway vector pGWL7 (VIB, Belgium) using the
364 Gateway LR clonase II enzyme mix (Thermo Fisher Scientific). We used all the cloning reactions
365 to transform the NEB Stable Competent *E. coli* (High Efficiency) (NEB, England). We left the
366 transformed cells to recover for one hour at 30°C in shaking conditions and then plated them on
367 LB plates containing the appropriate selecting antibiotic. We extracted the plasmid DNA
368 samples from the colonies using the QIAprep® Spin Miniprep kit (Qiagen) and sequence-verified
369 them using the Sanger method (Macrogen, The Netherlands). The sequences of the promoters
370 cloned in this study are listed in the Supplementary Table S6.

371

372 ***DNA constructs for trans-activation assay: Transcription factors***

373 We extracted RNA from leaves of *Solanum lycopersicum* cultivar M82 using RNeasy Mini kit
374 (Qiagen) followed by DNase I (Thermo Fisher Scientific) treatment. We synthesized cDNA using
375 RevertAid RT Reverse Transcription Kit (Thermo Fisher Scientific) together with random hexamer
376 primers (Thermo Fisher Scientific). We amplified the coding sequence of *SlWRKY71* using this
377 cDNA as template based on the gene model information of version ITAG2.4 (Supplementary
378 Figure S1), while the coding sequences of *SlMYB92* and *SlMYB41* were amplified from the
379 plasmids pENTR/D-TOPO previously cloned for overexpression. We amplified the CDS with
380 Phusion High-Fidelity DNA Polymerase (Thermo Fisher Scientific) and the primers listed in
381 Supplementary Table S7. We recombined the PCR products into the Gateway vector pDONR221
382 (Thermo Fisher Scientific) using the Gateway BP clonase II enzyme mix (Thermo Fisher Scientific)

383 and subsequently into the Gateway vector p2GW7 (Karimi *et al.*, 2002) using the Gateway LR
384 clonase II enzyme mix (Thermo Fisher Scientific). The reactions were transformed into
385 competent cells of *Escherichia coli* DH5α. The transformed cells were left to recover for one hour
386 at 37°C in shaking conditions and then plated on LB plates containing the appropriate selecting
387 antibiotic. The plasmid DNA samples were extracted and sequence-verified as described above.

388

389 ***Trans-activation assays***

390 We grew the material for protoplast-based trans-activation assays as follows. We stratified
391 *Arabidopsis thaliana* Col-0 plants for 4 days on soil:perlite mix 1:2 (Primasta BV, Asten, The
392 Netherlands) and then moved them to a growth chamber under short-day conditions (8 h light,
393 16 h dark; 20°C; 70% humidity) for a week to allow germination. The plants were then
394 transplanted and left to grow for 3 weeks. We isolated leaf mesophyll protoplasts using the tape
395 sandwich method (Wu *et al.*, 2009). We incubated the tapes containing the tissues in an
396 enzymatic solution [1% cellulase R-10 (Duchefa Biochemie), 0.25% macerozyme R-10 (Duchefa
397 Biochemie), 0.4 M mannitol, 20 mM KCl, 20 mM MES pH 5.8, 10 mM $CaCl_2$, 5 mM β-
398 mercaptoethanol, 0.1% BSA] in the dark with gentle agitation for two hours at room temperature.
399 We filtered the protoplasts through a 100 µm nylon mesh, washed them two times in W5 buffer
400 (154 mM NaCl, 125 mM $CaCl_2$, 5 mM KCl, 2 mM MES pH 5.8) and incubated them on ice for 30
401 minutes. We determined the protoplast number using a hemocytometer. We finally resuspended
402 the protoplasts in MMg solution (0.4 M mannitol, 15 mM $MgCl_2$, 5 mM MES pH 5.8). For each
403 biological replicate, we transfected 1-5 x 10^5 protoplasts with 10 µg of pDLUC15 plasmid
404 carrying the promoter sequence in combination with 3-5 µg of the vectors expressing the coding
405 sequence of the transcription factors of interest by adding a PEG solution (40% PEG 4000, 0.2 M
406 mannitol, 0.1 M $CaCl_2$). We incubated the reactions for 5 minutes; we stopped the transfections
407 with W5 buffer, and we washed them two times with W5 buffer. After transfection, we incubated
408 the protoplasts for 16-18 hours at room temperature in the dark, spun them down, and removed
409 the supernatant. We then detected the activity of the Firefly and Renilla luciferases with the Dual-
410 luciferase reporter assay system (Promega) and the GloMax 96 Microplate Luminometer
411 (Promega). We assayed two technical replicates for each biological replicate. The statistical
412 analysis was done as described in the legend of the figures.

413

414

415 **Results**

416 We explored the regulatory interactions that tomato exodermis-enriched TFs have with their
417 target genes in order to understand the suberin regulatory module in exodermis. We selected
418 three TFs, SlMYB92, SlMYB41 and SlWRKY71, as targets for this study, identified as exodermis-
419 enriched based on tomato root gene expression profiling by Cantó-Pastor *et al.* (2024) and Kajala
420 *et al.*(2021)(Figure 1A) and as regulators of suberin levels (SlMYB92 and SlMYB41, Cantó-Pastor
421 *et al.*, 2024). Using a translational fusion with GFP we confirmed that *SlMYB92* is expressed only
422 in the exodermis layer of tomato hairy roots (Figure 1B, Cantó-Pastor *et al.*, 2024), while
423 exodermis-specific promoter activities of *SlMYB41* and *SlWRKY71* were previously
424 demonstrated in Kajala *et al.* (2021).

425 The SlMYB TFs are homologous with known suberin regulators of Arabidopsis (Figure 1C).
426 Specifically, phylogenetic analysis of *SlMYB41* and *SlMYB92* with the closest Arabidopsis *MYB*

427 homologs, including 14 with described roles in suberization showed protein sequence similarity
428 with MYB subgroup S11 (*AtMYB41, AtMYB74, AtMYB102*) and S24 (*AtMYB93*, *AtMYB92* and
429 *AtMYB53*), respectively (Figure 1C).

430 For the WRKY TF, *SlWRKY71* was selected as a candidate due to its expression being
431 induced in drought, similarly to *SlMYB92, SlMYB41*, and suberin deposition (Cantó-Pastor *et al.*,
432 2024). Phylogenetic analysis of SlWRKY71 with homologous Arabidopsis WRKY proteins showed
433 that SlWRKY71 is closely related to AtWRKY71, AtWRKY8 and AtWRKY28, the latter of which has
434 previously been identified as a homolog of a candidate regulator of suberin biosynthesis in poplar
435 (Figure 1D, Supplementary Table S1) (Rains *et al.*, 2018). So, we asked if these two MYBs and
436 SlWRKY71 form a regulatory module to coordinate the expression of suberin biosynthesis genes
437 in the exodermis of tomato.

438 To identify the transcripts in the tomato root tip that are regulated by SlMYB92, SlMYB41
439 and SlWRKY71, we used both CRISPR/Cas9 induced knockouts and *p35S*-driven overexpression
440 constructs for all three TFs in tomato hairy root cultures (Ron *et al.*, 2014; Cantó-Pastor *et al.*,
441 2024). Additionally, the knockout and overexpression lines show if these TFs are necessary or
442 sufficient, respectively, for exodermal suberin deposition. For the MYB knockouts, we used our
443 previously published *Slmyb92*-ko and *Slmyb41*-ko lines that have reduced suberization of
444 tomato root exodermis (Cantó-Pastor *et al.*, 2024). The gene editing of *SlWRKY71* generated two
445 truncated versions of the protein *Slwrky71*-ko(4*)* and *Slwrky71*-ko(5) which we used in parallel in
446 our experiments (Supplementary Figure S1). For the overexpression constructs with the near
447 constitutive *35S* promoter, we included a C-terminal 3xFLAG tag and validated the hairy root lines
448 by protein accumulation as detected by anti-FLAG antibody (Supplementary Figure S2). For our
449 experiments, we selected the overexpression lines with the strongest TF accumulation
450 (Supplementary Figure S2).

451 Our first question about these lines was if they had altered exodermal deposition of
452 suberin or lignin. We set out to test the effect of the genetic perturbations by examining suberin
453 deposition in cross-sections of the ko and OX hairy root lines and comparing them to the control
454 (empty vector) hairy roots (Figure 2). As suberization in exodermis builds up gradually, starting
455 with a patchy pattern and building up to a fully suberized ring, we quantified our section data
456 accordingly. We scored whether cross-sections from individual roots had exodermis that was
457 non-suberized (0% of cells in a section), patchy ("early-suberized", <50% of cells in the section)
458 or more fully suberized pattern ("late suberized", >50% of cells in a section) (Figure 2A). For the
459 *Slmyb92*-ko and *Slmyb41*-ko*,* we saw reduction in exodermal suberisation when compared to
460 the empty vector control (Figure 2A-C), confirming that these two MYB TFs are necessary for
461 normal suberin deposition pattern in tomato exodermis. Conversely, the overexpressors of the
462 two *SlMYBs* had similar suberin deposition pattern as the control roots. This suggests that they
463 are not individually sufficient to affect suberization. In *SlWRKY*-OX, we observed an absence of
464 suberization in the exodermis (Figure 2A-C), while *Slwrky71*-kos did not affect the suberization.
465 This indicates a repressive role for SlWRKY71 in exodermal suberin deposition with potentially
466 other redundantly acting TFs. We then examined the lignin deposition in the exodermis of these
467 lines, and did not observe any changes to the deposition pattern (Supplementary Figure S3),
468 indicating that these TFs are likely to regulate only the suberin barrier deposition in exodermis.

469 To identify the potential target genes of SlMYB92, SlMYB41 and SlWRKY71, we performed
470 RNA sequencing (RNA-seq) of 1-cm root tips from hairy-root cultures of *Slmyb41*-ko, *SlMYB41*-
471 OX, *Slmyb92*-ko, *SlMYB92*-OX, *Slwrky71*-ko(4), *Slwrky71*-ko(5), *SlWRKY71*-OX and empty vector

472 control lines. Multidimensional scaling (MDS) analysis of the generated RNA-seq data
473 demonstrated the reproducibility of the biological replicates for each genotype. It also revealed
474 transcriptome similarities between the *Slmyb41*-ko and *Slmyb92*-ko lines, between the
475 *Slwrky71*-ko(4) and *Slwrky71*-ko(5) lines, and between the *SlWRKY71*-OX and *SlMYB41*-OX lines
476 (Figure 3A). For each line, differentially expressed genes (DEGs) were identified by comparing
477 them to the transcriptome data of control roots with an adjusted P-value threshold of 0.05 (Figure
478 3B). The list of DEGs identified in all the lines are summarized in Supplementary Dataset S1.
479 Perturbation of TF function by CRISPR-Cas9 led to notable changes in the transcriptome of hairy
480 roots, revealing 873, 624, 828, and 869 DEGs in *Slmyb4*-ko, *Slmyb92*-ko, *Slwrky71*-ko(4), and
481 *Slwrky71*-ko(5) knockout lines, respectively (Figure 3B). The same pattern was not observed in
482 the overexpressing lines, where 582 genes were identified in the *SlMYB92*-OX line, whereas
483 overexpressing *SlMYB41* and *SlWRKY71* led to the identification of a smaller number of DEGs,
484 165 and 126 respectively (Figure 3B). We compared the DEGs between the *Slmyb* ko lines and
485 found that 227 (53%) out of 426 down-regulated DEGs in *Slmyb41*-ko were also down-regulated
486 in *Slmyb92*-ko (Figure 3C). A similar pattern was observed in the list of upregulated genes in
487 *SlMYB*-OX lines (Figure 3D), where 76 (66%) out of 115 of up-regulated genes in *SlMYB41*-OX were
488 found to be upregulated in the *SlMYB92*-OX line (Figure 3D). The similarities observed between
489 the DEGs in both the OX and ko lines of *SlMYB41* and *SlMYB92* indicate an overlap in the gene
490 regulatory networks controlled by these two MYB TFs. We also compared the list of DEGs in the
491 two independent *Slwrky71*-ko lines and found that 60% and 54% of downregulated and
492 upregulated DEGs identified in *Slwrky71*-ko(5) line was found in the list of DEGs from *Slwrky71*-
493 ko(4) (Figure 3D). The major overlap between the DEG lists of the two independent *Slwrky71*-ko
494 lines indicates accurate identification of the genes regulated by this TF. For further analysis, we
495 consider the overlapping DEGs between the independent lines as the DEGs for *Slwrky71*-ko
496 (Figure 3D).

497 To identify the biological role of genes regulated by these TFs, we performed gene
498 ontology (GO) enrichment analysis and identified the metabolism-related GO terms enriched (q
499 value < 0.05) in the list of DEGs (Figure 3F). Lipid biosynthesis (GO:0008610) was found to be
500 enriched in the list of upregulated (UP) genes in *SlMYB92*-OX (Figure 3F). These genes include 3-
501 ketoacyl-CoA synthase (KCS)-encoding genes that are involved with the elongation of fatty-acids
502 (Li-Beisson *et al.*, 2010).

503 Interestingly, response to oxidative stress (GO:0006979) was found to be enriched in the
504 *SlMYB92*-OX upregulated list of DEGs (Figure 3D). This is likely due to the high number of genes
505 encoding peroxidases and catalases found in the OX lists of DEGs (Supplementary Figure S3). It
506 has been proposed that in addition to lignin deposition, peroxidases have a role in promoting the
507 formation of the suberin lamellae in tomato roots (Quiroga *et al.*, 2000; Serra and Geldner, 2022).
508 These results indicate that SlMYB92 is involved with the suberization of the tomato root
509 exodermis.

510 To further investigate if DEGs are involved in suberin biosynthesis in the exodermis, we
511 compared the list of DEGs to previously characterized tomato exodermis-enriched and tomato
512 root-expressed suberin biosynthesis genes (Kajala *et al.*, 2021; Cantó-Pastor *et al.*, 2024) (Figure
513 3G). We identified a significant overlap ($p < 0.01$) between the DEGs in *Slmyb41*-ko*, Slmyb92*-ko*,*
514 *SlMYB92*-OX*, Slwrky71*-ko(4), and *Slwrky71*-ko(5) with the previously annotated tomato
515 exodermis-enriched genes (Kajala *et al.*, 2021) (Figure 3G). Additionally, we found a significant
516 overlap between the DEGs in *SlMYB92*-OX and *SlMYB41*-OX with the previously described list of
517 tomato root suberin-related genes (Cantó-Pastor *et al.*, 2024). Finally, to determine the extent to

518 which these TFs regulate genes involved in the distinct steps of suberin biosynthesis, we
519 compared the list of DEGs to the genes associated with fatty acid (FA) (very long chain FA
520 biosynthesis I & II) and suberin biosynthesis (suberin monomers biosynthesis and esterified
521 suberin biosynthesis) pathways in the tomato Plant Metabolic Network (PMN)
522 (https://plantcyc.org/databases/tomatocyc/4.0). We observed a significant overlap between the
523 DEGs in *SlMYB41*-OX and *SlMYB92*-OX with the FA and suberin-related pathways (Figure 3H).
524 This finding suggests that MYB TFs promote the suberization of the tomato root exodermis by
525 enhancing the expression of genes involved in the precursors and monomers of suberin
526 biosynthesis. Notably, some of these genes encode for key enzymes of the suberin biosynthesis
527 pathway, and enzymes such as Aliphatic Suberin Feruloyl Transferase / ω-HYDROXYACID/FATTY
528 ALCOHOL HYDROXY-CINNAMOYL TRANSFERASE (ASFT/FHT) (*Solyc03g097500.3.1*) (Serra and
529 Geldner, 2022; Cantó-Pastor *et al.*, 2024) and glycerol-3-phosphate acyltransferase 4 (GPAT4)
530 (*Solyc01g094700.3.1* and other GPATs, *Solyc03g097500.3.1*, *Solyc09g014350.3.1*) (Feng *et al.*,
531 2022; Serra and Geldner, 2022). Altogether, our results support SlMYB92 and SlMYB41 as
532 regulators of the suberin biosynthesis program in the tomato root exodermis.

533 Our RNA-seq analysis also suggests an antagonistic role between the two SlMYBs and
534 SlWRKY71 transcription factors in regulating the suberin biosynthesis program in tomato roots.
535 For instance, 107 out of 371 upregulated genes (FDR < 0.05 and logFC > 0) in *SlMYB92*-OX were
536 also upregulated in *Slwrky71*-ko (Figure 4A). Furthermore, similar to the peroxidase and catalase
537 genes (Supplementary Figure S4), many suberin biosynthesis-related genes upregulated in
538 *SlMYB92*-OX and *SlMYB41*-OX exhibited lower fold-change levels in *SlWRKY71*-OX (Figure 4B).
539 These results suggest that these SlMYBs primarily act as positive regulators of the suberin
540 biosynthesis program in the tomato root exodermis, while SlWRKY71 functions as a repressor of
541 exodermis suberization. Moreover, these results indicate that these TFs may balance each
542 other's actions to fine-tune the expression of suberin biosynthesis genes in the tomato root
543 exodermis.

544 To further test the function of these TFs in the transcription of their target genes, we
545 performed transactivation assays in Arabidopsis mesophyll protoplasts using individual TFs and
546 all their combinations. A construct overexpressing GFP was used to establish a baseline for the
547 assay. A schematization of the constructs used is shown in Figure 4C. For these assays we tested
548 the promoter regions of the two *SlMYBs* and of *SlWRKY71,* to see whether they regulate their own
549 expression, in addition to three other candidate genes selected for their involvement in the
550 suberin biosynthesis pathway and their transcriptional response in the transgenic hairy roots
551 (Supplementary Figure S4). Among the different promoter regions used, only
552 *Solyc03g115960.3.1* (*GDSL esterase/lipase38* (*SlGELP38*)), *Solyc07g056320.4.1* (*Glycerol-3-*
553 *phosphate acyltransferase*) and *Solyc01g094700.5.1* (*SlGPAT4*) showed a positive
554 transactivation (Figure 4D, Supplementary Figure S5). Specifically, *SlGPAT4* was transactivated
555 by SlMYB92 alone and when in combination with the other two TFs. On the other hand, *SlGELP38*
556 and *Solyc07g056320.4.1* were transactivated by both SlMYB92 and SlMYB41 and their
557 combination, but not by SlWRKY71 (Figure 4D). When SlWRKY71 was combined with either one
558 or with both MYBs, it seemed to act like a repressor of promoter activity (Figure 4D). This suggests
559 that SlMYB92 and SlMYB41 are positive regulators of these genes while SlWRKY71 counteracts
560 the function of the two SlMYBs (Figure 4). Overall, it appears that the MYBs are direct activators
561 of promoters of suberin-related genes and their effect may be additive, while SlWRKY71 can act
562 as an activator or an inhibitor of promoter activity depending on the promoter and context of
563 other TFs present.

564

565 **Discussion**

566 ***SlMYB92 and SlMYB41 are positive regulators of the suberin biosynthesis program in tomato***
567 ***root exodermis***

568 In Arabidopsis roots, suberin accumulates in the endodermal cell layer, whereas in tomato,
569 suberization occurs in the exodermal cell layer. Despite this spatial distinction, it has been
570 shown that both processes are controlled by similar components (Cantó-Pastor *et al.*, 2024).
571 Several reports have shown the role of MYB TFs in the control of the suberization in the root
572 endodermal cell layer. In Arabidopsis, several MYB TFs, including AtMYB41, AtMYB53, AtMYB92,
573 and AtMYB93, have been shown to be involved in the biosynthesis of suberin in the root
574 endodermal cell layer (Shukla *et al.*, 2021). Additionally, 13 key MYB TFs were identified in
575 transcriptional regulatory network to control the suberization and lignification in the Arabidopsis
576 endodermis (Xu *et al.*, 2022*b*). In this sense, it is likely that MYB TFs would also play an important
577 role in the suberization of the root exodermis in tomato. Here we provide several lines of evidence
578 that show that SlMYB92 and SlMYB41 can act as positive regulators of suberin biosynthesis by
579 regulating the expression of several genes involved with the different steps of suberin
580 biosynthesis in tomato roots. First, as previously reported, *SlMYB92* and *SlMYB41* are expressed
581 primarily at the exodermal cell layer of the tomato root (Figure 1) (Kajala *et al.*, 2021; Cantó-
582 Pastor *et al.*, 2024). Second, perturbations of *SlMYB92* and *SlMYB41* coding sequences by
583 CRISPR/Cas9 resulted in a significant delay in suberin deposition in the tomato root exodermis
584 (Figure 2, Cantó-Pastor *et al.*, 2024). Third, overexpression of *SlMYB92* and *SlMYB41* in tomato
585 hairy root cultures resulted in the upregulation of several genes involved with suberin
586 biosynthesis (Supplementary Dataset S2). However, we did not observe increased accumulation
587 of suberin in the *SlMYB*-OX lines, indicating that they might work together to upregulate the
588 complete suberin biosynthesis and deposition pathways. Fourth, we showed that promoters of
589 suberin biosynthesis genes are transactivated by SlMYB92 and SlMYB41 in Arabidopsis leaf
590 protoplasts (Figure 4D), indicating direct activation of the promoter activity. Together, our results
591 provide strong evidence that SlMYB92 and SlMYB41 act as positive regulators of suberin
592 biosynthesis in the tomato root exodermis.

593 Given the challenges of generating transgenic tomato plants, our genetic perturbations
594 were done with the tomato hairy root cultures and transactivation assays in Arabidopsis leaf
595 protoplasts, which introduces the caveats of using model systems that are different from the
596 tomato embryonic roots. We observed lower levels and higher variation of exodermal
597 suberization in the tomato hairy root cultures compared to primary roots (Kajala *et al.*, 2021;
598 Cantó-Pastor *et al.*, 2024). We did not observe *SlMYB* overexpressors driving increased
599 suberization unlike previously observed for other species (Kosma *et al.*, 2014; Shukla *et al.*, 2021;
600 Chen *et al.*, 2024). This could be due to inadvertent selection towards weakly suberizing alleles.
601 If the SlMYBs were sufficient to drive suberization, their effect expressed under the near-
602 constitutive 35S promoter could lead to inhibition of root growth, and hence not being selected
603 for hairy root cultures. Additionally, the heterologous trans-activation assay might be affected by
604 the factors present in the heterologous tissue of a different species. While these challenges may
605 affect the interpretation of the results, the different lines of inquiry support each other and are
606 consistent with the Arabidopsis literature for the endodermis.

607

608 ***SlMYB92 and SlMYB41 regulate genes involved in suberin biosynthesis and deposition***

609 Suberin is a highly heterogeneous biopolymer comprised of a variety of aliphatic long chain fatty
610 acids and their oxidized derivatives, glycerol and ferulic acid (Shukla and Barberon, 2021; Serra
611 and Geldner, 2022). Due to its biochemical complexity, the action of several enzymes that
612 operate in distinct compartments of the cell needs to be highly coordinated. Here, we show that
613 SlMYB92 and SlMYB41 can regulate the expression of several genes involved in the many steps
614 required for the biosynthesis of suberin monomers, their transport and polymerization in the
615 apoplast (summarized in Supplementary Dataset S2). The precursors of suberin monomers are
616 produced via two major biochemical pathways: very-long-chain fatty acid (VLCFA) and
617 phenylpropanoid biosynthesis pathways (Shukla and Barberon, 2021). The fatty-acid elongase
618 (FAE) complex catalyzes the elongation of acyl-CoA into VLCFA. Within this complex, the
619 ketoacyl-CoA synthases (KCS) enzyme carries out the rate-limiting step (Haslam and Kunst,
620 2013; Batsale *et al.*, 2021; Serra and Geldner, 2022). Here we showed that *SlKCS1*
621 (*Solyc10g009240.3.1*), *SlKCS6* (*Solyc02g085870.3.1*) and *SlKCS20* (*Solyc03g005320.3.1* and
622 *Solyc09g083050.3.1*) were up-regulated in the *SlMYB92*-OX line while *SlKCS11*
623 (*Solyc08g067410.2.1*) was down-regulated in *Slmyb41*-ko and *Slwrky71*-ko lines. These VLFAs
624 are further modified by laccases (LACSs) and CYTOCHROME P450s (CYPs) (Serra and Geldner,
625 2022). We found three LACS encoding genes to be upregulated in *SlMYB92*-OX
626 (*Solyc04g011900.4.1, Solyc05g052340.4.1, Solyc06g082240.2.1/SlLAC3-like*) and one
627 downregulated in *Slmyb41*-ko (*Solyc06g050530.3.1/SlLAC12-like*). Notably, tomato orthologues
628 of *CYP86A1* (*Solyc06g076800.3.1*) and *CYP86B1* (*Solyc02g014730.3.1*), two main CYPs involved
629 with the ω-oxidation of FAs and endodermis suberization in Arabidopsis (Li *et al.*, 2007; Höfer *et*
630 *al.*, 2008; Compagnon *et al.*, 2009) were upregulated in hairy-roots overexpressing SlMYB92
631 (Supplementary Dataset S2). Knock-out mutations in the latter (SlCYP86B1) resulted in a
632 reduction of exodermis suberization in tomato hairy roots (Cantó-Pastor *et al.*, 2024).

633 In the final steps of suberin monomer biosynthesis, a feruloyl transferase (ASFT/FHT) and
634 GPATs are involved with the feruloylation and glyceration of suberin precursors, respectively
635 (Serra and Geldner, 2022). It has been previously shown that knocking down *SlASFT* and *SlGPAT4*
636 in tomato hairy roots resulted in dramatic reduction on exodermis suberization (Cantó-Pastor *et*
637 *al.*, 2024). We found that *SlASFT* (*Solyc03g097500.3.1*) and *SlGPAT6* (*Solyc03g097500.3.1*) to be
638 upregulated in *SlMYB92*-OX while *SlGPAT4* (*Solyc01g094700.5.1*) was found upregulated in
639 *SlMYB92*-OX and *SlMYB41*-OX (Supplementary Dataset S2)**.** The transport of suberin monomers
640 to the apoplast is mediated by lipid transfer proteins (LTPs) and ATP-binding cassette
641 transporters of the subfamily G (ABCG) (Shukla and Barberon, 2021). In Arabidopsis, AtLTPg15
642 was found to be important for the transport of suberin monomers export to the seed coat (Lee
643 and Suh, 2018). Interestingly, we observed that the tomato orthologue of *AtLTPg15*
644 (*Solyc09g065430.4.1*) was upregulated by overexpressing *SlMYB92* and *SlMYB41*
645 (Supplementary Dataset S2). Additionally, two ABCG-encoding genes (*Solyc03g019760.4.1* and
646 *Solyc05g054890.4.1/SlABCG2*) were upregulated in *SlMYB92*-OX, and another *ABCG* gene
647 (*Solyc05g051530.5.1*) was downregulated in *Slmyb92*-ko and *Slmyb41*-ko but upregulated in
648 *SlMYB92*-OX compared to the control hairy root culture.

649 After the transport of suberin monomers, the GDSL-type Esterase/Lipase Protein (GELP)
650 family are involved with the suberin polymerization in the apoplastic space. A recent study has
651 shown that quintuple *GELP* mutants (*gelp22-38-49-51-96*) have drastic reduction in endodermis
652 suberization (Ursache *et al.*, 2021). We observed that a *GELP* gene
653 (*Solyc03g115960.3.1/SlGELP38*) previously identified as specifically expressed in the exodermal

654 cell layer (Kajala *et al.*, 2021; Cantó-Pastor *et al.*, 2024) was upregulated by the overexpression
655 of *SlMYB92* (Supplementary Dataset S2). Additionally, four other GELP-encoding genes
656 (*Solyc02g070610.3.1, Solyc10g085170.3.1, Solyc11g051060.2.1, Solyc10g076740.3.1*) were
657 downregulated in the *Slmyb41*-ko or *Slmyb92*-ko (Supplementary Dataset S2).

658 Altogether, these results show that SlMYB92 and SlMYB41 are major regulators of
659 exodermis suberization by promoting the expression of genes involved with the biosynthesis,
660 transport and polymerization of suberin in tomato roots.

661

662 ***The role of MYBs in gene regulation***

663 MYBs are among the largest families of TFs discovered in plants, extensively characterized for
664 their role in regulating responses to various abiotic stresses, such as drought and high salinity.
665 Additionally, they play a pivotal role in regulating the biosynthetic pathways of secondary
666 metabolites, including anthocyanins, proanthocyanidins, flavonols, lignin, and suberin (Cao *et*
667 *al.*, 2020; Wang *et al.*, 2021; Xu *et al.*, 2022*b*). MYBs can carry out their regulatory functions as
668 monomers, homodimers, heterodimers or as part of protein complexes (Pireyre and Burow,
669 2015). For example, in the anthocyanin and proanthocyanidin pathways, MYBs interact with
670 bHLH TFs, and, together with a WD40 protein, form the MBW complex, which regulates the
671 transcription of biosynthetic genes (Xu *et al.*, 2015). MYBs that participate in the MBW complex
672 contain a bHLH-binding motif in their sequence, [DE]Lx2[RK]x3Lx6Lx3R, responsible for the
673 interaction between MYBs and bHLH (Zimmermann *et al.*, 2004). The MYB sequences studied
674 here do not contain this motif, suggesting that SlMYB92 and SlMYB41 do not require an MBW
675 complex to activate transcription. In fact, the suberin biosynthetic pathway is primarily regulated
676 by MYB, NAC, and WRKY TFs (Woolfson *et al.*, 2022). This observation aligns with our evidence
677 that the two MYBs examined in this study can transactivate gene expression independently of
678 bHLH transcription factors (Figure 4D).

679 The primary role of both MYBs seems to be regulating the expression of biosynthetic
680 genes, with minimal impact on the regulation of other TFs (Supplementary Dataset S2). For
681 instance, overexpression of *SlMYB41* leads to the upregulation of only one WRKY TF
682 (*Solyc03g095770.3.1*, *AtWRKY70*), while *SlMYB92* overexpression results in the upregulation of
683 just two WRKY TFs (*Solyc01g095630.3.1* and *Solyc09g015770.3.1)*. Notably, *SlMYB41*
684 overexpression does not affect the upregulation of any MYB-encoding gene, whereas *SlMYB92*
685 overexpression induces the upregulation of four MYBs (*Solyc03g093930.5.1*,
686 *Solyc06g075660.4.1*, *Solyc06g065100.3.1*, *Solyc02g082040.3.1*). Additionally, in the *Slmyb41*
687 and *Slmyb92* ko lines, only three MYBs were found to be downregulated (*Solyc05g007160.3.1*,
688 *Solyc02g088190.5.1*, *Solyc09g090790.3.1*). This is similar to the multi-hierarchical regulatory
689 network for Arabidopsis endodermal suberin and lignin proposed by Xu *et al.*, (2022*b*), where
690 AtMYB92 and AtMYB41 are in separate tiers and distinct branches of the network. Conversely to
691 our data, in the network by Xu and colleagues, AtMYB41 is more of a hub coordinator and would
692 be expected to induce higher number of DEGs when mutated or induced, while AtMYB92 is on
693 the last tier, with low impact on other TFs. It is likely that the way in which suberin GRN is
694 connected differs between species, cells and tissues, even if they utilize orthologous MYB TFs.

695 Moreover, the TFs studied here do not exhibit self-activation and do not appear to
696 regulate each other's expression (Supplementary Figure S4). This suggests that other MYBs may
697 be responsible for their regulation. Additionally, given that the ko lines of both *SlMYB41* and

698 *SlMYB92* had reduced suberin (Cantó-Pastor *et al.*, 2024), it indicates that the *SlMYBs* are
699 working as necessary but not directly connected nodes in an exodermal suberin GRN.
700 Alternatively, it is possible that some of these regulatory interactions are dependent on e.g.
701 having the right ratio of binding partners in a MYB heterodimer. Further studies are required to
702 elucidate the regulatory mechanisms upstream the TFs investigated in this study.

703

704 ***Antagonistic interaction of MYBs and WRKYs in regulating suberin***

705 Together with MYBs, WRKYs appear as one of the most relevant TF families involved in suberin
706 biosynthesis in several species and tissue types (Lashbrooke *et al.*, 2016). WRKYs modulate gene
707 expression by binding to W-box *cis*-regulatory elements of stress-induced genes, and control
708 mainly senescence, stress and defense responses (Eulgem *et al.*, 2000; Rushton *et al.*, 2010).

709 Expression of a WRKY TF in rice roots (LOC_Os01g53260), together with MYBs and other
710 TFs, have been shown to enhanced radial oxygen loss (ROL) barrier formation (including suberin
711 and lignin), and WRKY *cis*-regulatory elements were enriched in the promoters of the majority of
712 upregulated genes in this tissue (Shiono *et al.*, 2014). Arabidopsis MYB107 was found to be a
713 positive regulator of suberin biosynthesis genes during seed development, and WRKYs were
714 among the TFs that were either co-expressed with *MYB107* or co-supressed in *myb107* (Gou *et*
715 *al.*, 2017). Among the co-expressed partners were *AtWRKY56* (*At1g64000*) and *AtWRKY43*
716 (*At2g46130*) (Supplementary Table S1, Gou *et al.*, 2017). Furthermore, WRKYs were listed as
717 candidate for suberin biosynthesis and cork regulation in cork oak (*Quercus suber*) together with
718 MYBs, and a homolog of *AtWRKY43* was among the candidate with high fold change values (Soler
719 *et al.*, 2007). Homologs of *AtWRKY65*, *AtWRKY43*, *AtWRKY6* and *AtWRKY28* were also among the
720 transcripts with the highest fold change in poplar bark, being potential candidates for
721 biosynthesis and regulation of poplar suberin (Rains *et al.*, 2018).

722 The WRKY and MYB TFs interact also in defense response mechanisms in a complex way,
723 exhibiting both positive and negative interactions. Barco and Clay (2019) observed two
724 overlapping regulatory functions for AtWRKY33 and AtMYB51 in the expression of defense-
725 responsive specialize metabolism genes: while AtWRKY33 activated and AtMYB51 repressed the
726 expression of one biosynthetic enzyme (CYP82C2), both TFs activate the expression of other two
727 enzymes (CYP79B2 and CYP79B3). According to the authors, this indicates a hierarchical TF
728 cascade were AtWRKY33 function as the condition-dependent master regulator and AtMYB51 as
729 the dual functional regulator (Barco and Clay, 2019). Interestingly, the authors also found that
730 AtWRKY33 and AtMYB51 do not co-localize on the promoters of these enzymes, suggesting that
731 these TFs likely alternate in binding the promoter regions.

732 There are also examples of WRKY and MYB TFs working together as an activating
733 complex. One such example is the transcription factor VqWRKY53 in Chinese wild grape (*Vitis*
734 *quinquangularis*), induced by pathogen infection, forms a transcriptional complex with VqMYB14
735 and VqMYB15. This complex positively regulates stilbene accumulation, a phytoalexin produced
736 in response to abiotic and biotic stresses, thereby contributing to disease resistance (Wang *et*
737 *al.*, 2020*a*).

738 Here, we have uncovered an antagonistic interaction between inhibitory SlWRKY71 and
739 activating SlMYB41 and SlMYB92. The genetic perturbations of *SlWRKY71* indicated that
740 SlWRKY71 is a repressor of tomato exodermal suberin (Figure 2), while SlMYB92 and SlMYB41
741 are necessary for tomato exodermal suberin deposition (Cantó-Pastor *et al.*, 2024). The lack of

742 statistically significant phenotype for *SlWRKY71*-kos may be explained either the mutation
743 having a subtle effect on the suberin pattern at the sampled location, or by other, redundant TFs
744 having the same antagonistic role.

745 Furthermore, we showed that these TFs antagonistically regulate expression of suberin-
746 related genes in tomato exodermis (Figure 4). We observed an overlap of DEGs induced by
747 *SlMYB41* and *SlMYB92* overexpression and *Slwrky71* knockout, indicating that the same target
748 genes are activated by SlMYBs as are repressed by SlWRKY71 (Figure 4A). We also observed that
749 the *SlWRKY71*-OX DEGs had a contrasting behavior to the *SlMYB*-OX lines (Figure 4B). Finally, we
750 showed that the presence of SlWRKY71 with the two SlMYBs prevents their ability to induce
751 promoter activity in Arabidopsis protoplasts for two target promoters (Figure 4D).

752 The potential mechanisms of this MYB-WRKY antagonism could be by interactions at
753 different levels. As described in the examples above, it could arise from direct MYB-WRKY
754 binding, or by competitive binding of WRKY and the MYB TFs on the target promoters.
755 Additionally, SlWRKY71 mechanism of repression can also be amplified through the repression
756 of other WRKY TFs. For instance, we found that *SlWRKY41* and *SlWRKY70* were up-regulated in
757 *Slwrky71*-ko lines (Supplementary Dataset S2). These two SlWRKY TFs were found to be
758 upregulated in the SlMYB overexpressing lines (Supplementary Dataset S2). This suggests that
759 there may be downstream TFs regulated antagonistically by SlWRKY71 and the two SlMYBs.

760 Interestingly, *SlWRKY71* expression is drought-induced (Cantó-Pastor *et al.*, 2024)
761 alongside with the *SlMYBs* and suberin deposition. Why would both activators and repressors of
762 the suberin gene expression be induced simultaneously in tomato exodermis? This might
763 represent a pre-set pulse in suberin biosynthetic gene expression to ensure that available
764 resources are not overspent on making too much suberin. These nuances arising from
765 antagonistic interactions in the exodermis suberin GRNs may set a complex challenge for
766 endeavours of manipulating suberin levels for improved drought resilience and sequestration of
767 carbon dioxide from the atmosphere into suberin. The future challenges involve understanding
768 the importance of the repressors of suberin in plant fitness and characterizing the network more
769 fully.

770

771

772 **Supplementary files:**

773 Dataset S1: Differentially Expressed Genes (DEGs) in tomato hairy-root cultures.

774 Dataset S2: Combined summary of DEGs.

775 Figure S1: SlWRKY71 sequences and truncations generated with gene editing,

776 Figure S2: TF overexpression is detected on protein level.

777 Figure S3: Exodermal lignin is unaffected by *SlMYB92*, *SlMYB41* and *SlWRKY71*
778 perturbations

779 Figure S4: Expression of peroxidases and catalases is affected in TF knockouts and
780 overexpressors.

781 Figure S5: Transactivation assays of *SlMYB92*, *SlMYB41* and *SlWRKY71* promoters in
782 protoplasts of *A. thaliana*.

783 Table S1: *MYB41*, *MYB92* and *WRKY71* homologs from Arabidopsis and summary of their
784 potential roles in regulating suberization.

785 Table S2: Primers used to create the overexpression constructs.

786 Table S3: guide RNAs (gRNAs) designed to knock out *SlWRKY71*.

787 Table S4: List of promoters used in trans-activation assays.

788 Table S5: Primers used to amplify the promoters used for transactivation assays.

789 Table S6: Genomic sequences of promoters cloned for transactivation assays.

790 Table S7: Primers used to amplify coding regions of *SlMYB92*, *SlMYB41* and *SlWRKY71* for
791 transactivation assays.

792

793 **Acknowledgements**

794 We thank Tuğba Akyüz, Chrysa Pantazopoulou, Linge Li, Gijs van Asselt, Chenyun Hsieh, and
795 Alise Žvigule for experimental assistance, and Kevin Morimoto for critical reading of the
796 manuscript. The M82 seeds were provided by C.M. Rick Tomato Genetics Resource Center.

797

798 **Author contributions**

799 KK, SMB: Conceptualization, Supervision, and Funding Acquisition

800 LJ, SB, MASA, RK, ACP: Investigation

801 LJ, SB, MASA, RK: Data Curation, Formal Analysis, Visualization.

802 KK, LJ, SB, MASA, RK: Writing – Original Draft.

803 All authors: Writing – Review & Editing.

804 All authors read and have approved the final manuscript.

805

806 **Conflict of interest**

807 No conflict of interest declared.

808

809 **Funding statement**

810 This work was supported by Marie Skłodowska Curie Actions Reintegration fellowship 790057 to
811 KK, Netherlands Organization for Scientific Research (NWO) VIDI grant number VI.Vidi.193.104
812 to KK, and ACP and SMB by NSF PGRP IOS-2119820.

813

814 **Data availability**

815 The RNA sequencing data from this study are openly available in NCBI GEO repository reference
816 number GSE278561.

References:

Artur MAS, Kajala K. 2021. Convergent evolution of gene regulatory networks underlying plant adaptations to dry environments. Plant, cell & environment **44**, 3211–3222.

Barberon M. 2017. The endodermis as a checkpoint for nutrients. The new phytologist **213**, 1604–1610.

Barberon M, Vermeer JEM, De Bellis D, *et al.* 2016. Adaptation of root function by nutrient-induced plasticity of endodermal differentiation. Cell **164**, 447–459.

Barco B, Clay NK. 2019. Hierarchical and dynamic regulation of defense-responsive specialized metabolism by WRKY and MYB transcription factors. Frontiers in plant science **10**, 1775.

Bari VK, Nassar JA, Kheredin SM, Gal-On A, Ron M, Britt A, Steele D, Yoder J, Aly R. 2019. CRISPR/Cas9-mediated mutagenesis of CAROTENOID CLEAVAGE DIOXYGENASE 8 in tomato provides resistance against the parasitic weed Phelipanche aegyptiaca. Scientific reports **9**, 11438.

Batsale M, Bahammou D, Fouillen L, Mongrand S, Joubès J, Domergue F. 2021. Biosynthesis and functions of very-long-chain fatty acids in the responses of plants to abiotic and biotic stresses. Cells (Basel, Switzerland) **10**, 1284.

Birkenbihl RP, Diezel C, Somssich IE. 2012. Arabidopsis WRKY33 is a key transcriptional regulator of hormonal and metabolic responses toward Botrytis cinerea infection. Plant physiology **159**, 266–285.

Bray NL, Pimentel H, Melsted P, Pachter L. 2016. Near-optimal probabilistic RNA-seq quantification. Nature biotechnology **34**, 525–527.

Cantó-Pastor A, Kajala K, Shaar-Moshe L, *et al.* 2024. A suberized exodermis is required for tomato drought tolerance. Nature plants **10**, 118–130.

Cao Y, Li K, Li Y, Zhao X, Wang L. 2020. MYB transcription factors as regulators of secondary metabolism in plants. Biology **9**, 61.

Capote T, Barbosa P, Usié A, Ramos AM, Inácio V, Ordás R, Gonçalves S, Morais-Cecílio L. 2018. ChIP-Seq reveals that QsMYB1 directly targets genes involved in lignin and suberin biosynthesis pathways in cork oak (Quercus suber). BMC plant biology **18**.

Chen X, Liu K, Luo T, Zhang B, Yu J, Ma D, Sun X, Zheng H, Xin B, Xia J. 2024. Four MYB transcription factors regulate suberization and non-localized lignification at the root endodermis in rice. The plant cell doi: 10.1093/plcell/koae278.

Cohen H, Fedyuk V, Wang C, Wu S, Aharoni A. 2020. SUBERMAN regulates developmental suberization of the Arabidopsis root endodermis. The Plant journal: for cell and molecular biology **102**, 431–447.

Compagnon V, Diehl P, Benveniste I, Meyer D, Schaller H, Schreiber L, Franke R, Pinot F. 2009. CYP86B1 is required for very long chainω-hydroxyacid andα,ω-dicarboxylic acid synthesis in root and seed suberin polyester. Plant physiology **150**, 1831–1843.

Doblas VG, Geldner N, Barberon M. 2017. The endodermis, a tightly controlled barrier for nutrients. Current opinion in plant biology **39**, 136–143.

Du H, Liang Z, Zhao S, Nan M-G, Tran L-SP, Lu K, Huang Y-B, Li J-N. 2015. The evolutionary history of R2R3-MYB proteins across 50 eukaryotes: New insights into subfamily classification and expansion. Scientific reports **5**.

Dubos C, Stracke R, Grotewold E, Weisshaar B, Martin C, Lepiniec L. 2010. MYB transcription factors in Arabidopsis. Trends in plant science **15**, 573–581.

Ejiri M, Shiono K. 2019. Prevention of radial oxygen loss is associated with exodermal suberin along adventitious roots of annual wild species of Echinochloa. Frontiers in plant science **10**, 254.

Eulgem T, Rushton PJ, Robatzek S, Somssich IE. 2000. The WRKY superfamily of plant transcription factors. Trends in plant science **5**, 199–206.

Fauser F, Schiml S, Puchta H. 2014. Both CRISPR/Cas‐based nucleases and nickases can be used efficiently for genome engineering in *Arabidopsis thaliana*. The Plant journal: for cell and molecular biology **79**, 348–359.

Feng T, Wu P, Gao H, Kosma DK, Jenks MA, Lü S. 2022. Natural variation in root suberization is associated with local environment in *Arabidopsis thaliana*. The new phytologist **236**, 385–398.

Figueiredo R, Portilla Llerena JP, Kiyota E, Ferreira SS, Cardeli BR, de Souza SCR, dos Santos Brito M, Sodek L, Cesarino I, Mazzafera P. 2020. The sugarcane ShMYB78 transcription factor activates suberin biosynthesis in Nicotiana benthamiana. Plant molecular biology **104**, 411–427.

Goodstein DM, Shu S, Howson R, *et al.* 2012. Phytozome: a comparative platform for green plant genomics. Nucleic acids research **40**, D1178-86.

Gou M, Hou G, Yang H, Zhang X, Cai Y, Kai G, Liu C-J. 2017. The MYB107 transcription factor positively regulates suberin biosynthesis. Plant physiology **173**, 1045–1058.

Han X, Wei X, Lu W, Wu Q, Mao L, Luo Z. 2022. Transcriptional regulation of KCS gene by bZIP29 and MYB70 transcription factors during ABA-stimulated wound suberization of kiwifruit (Actinidia deliciosa). BMC plant biology **22**.

Haslam TM, Kunst L. 2013. Extending the story of very-long-chain fatty acid elongation. Plant science: an international journal of experimental plant biology **210**, 93–107.

Höfer R, Briesen I, Beck M, Pinot F, Schreiber L, Franke R. 2008. The Arabidopsis cytochrome P450 CYP86A1 encodes a fatty acid ω-hydroxylase involved in suberin monomer biosynthesis. Journal of experimental botany **59**, 2347–2360.

Huang X, Li Y, Chang Z, *et al.* 2024. Regulation by distinct MYB transcription factors defines the roles of *OsCYP86A9* in anther development and root suberin deposition. The Plant journal: for cell and molecular biology **118**, 1972–1990.

Jo L, Kajala K. 2024. ggPlantmap: an open-source R package for the creation of informative and quantitative ggplot maps derived from plant images. Journal of experimental botany doi: 10.1093/jxb/erae043.

Jo L, Pelletier JM, Hsu S-W, Baden R, Goldberg RB, Harada JJ. 2020. Combinatorial interactions of the LEC1 transcription factor specify diverse developmental programs during soybean seed development. Proceedings of the National Academy of Sciences of the United States of America **117**, 1223–1232.

Kajala K, Gouran M, Shaar-Moshe L, *et al.* 2021. Innovation, conservation, and repurposing of gene function in root cell type development. Cell **184**, 5070.

Karimi M, Inzé D, Depicker A. 2002. GATEWAY vectors for Agrobacterium-mediated plant transformation. Trends in plant science **7**, 193–195.

Karkute SG, Gujjar RS, Rai A, Akhtar M, Singh M, Singh B. 2018. Genome wide expression analysis of WRKY genes in tomato (Solanum lycopersicum) under drought stress. Plant gene **13**, 8–17.

Kawa D, Thiombiano B, Shimels MZ, *et al.* 2024. The soil microbiome modulates the sorghum root metabolome and cellular traits with a concomitant reduction of Striga infection. Cell reports **43**, 113971.

Kosma DK, Murmu J, Razeq FM, Santos P, Bourgault R, Molina I, Rowland O. 2014. AtMYB41 activates ectopic suberin synthesis and assembly in multiple plant species and cell types. The Plant journal: for cell and molecular biology **80**, 216–229.

Kreszies T, Eggels S, Kreszies V, Osthoff A, Shellakkutti N, Baldauf JA, Zeisler-Diehl VV, Hochholdinger F, Ranathunge K, Schreiber L. 2020. Seminal roots of wild and cultivated barley differentially respond to osmotic stress in gene expression, suberization, and hydraulic conductivity. Plant, cell & environment **43**, 344–357.

Krishnamurthy P, Vishal B, Ho WJ, Lok FCJ, Lee FSM, Kumar PP. 2020. Regulation of a cytochrome P450 gene *CYP94B1* by WRKY33 transcription factor controls apoplastic barrier formation in roots to confer salt tolerance. Plant physiology **184**, 2199–2215.

Krueger F. 2015. A wrapper tool around Cutadapt and FastQC to consistently apply quality and adapter trimming to FastQ files 516. **517**.

Kumar A, Sichov N, Bucki P, Miyara SB. 2023. SlWRKY16 and SlWRKY31 of tomato, negative regulators of plant defense, involved in susceptibility activation following root-knot nematode Meloidogyne javanica infection. Scientific reports **13**.

Lashbrooke J, Cohen H, Levy-Samocha D, *et al.* 2016. MYB107 and MYB9 homologs regulate suberin deposition in angiosperms. The plant cell **28**, 2097–2116.

Lee SB, Suh M-C. 2018. Disruption of glycosylphosphatidylinositol-anchored lipid transfer protein 15 affects seed coat permeability in Arabidopsis. The Plant journal: for cell and molecular biology **96**, 1206–1217.

Legay S, Guerriero G, André C, Guignard C, Cocco E, Charton S, Boutry M, Rowland O, Hausman J-F. 2016. MdMyb93 is a regulator of suberin deposition in russeted apple fruit skins. The new phytologist **212**, 977–991.

Letunic I, Bork P. 2016. Interactive tree of life (iTOL) v3: an online tool for the display and annotation of phylogenetic and other trees. Nucleic acids research **44**, W242–W245.

Li Y, Beisson F, Ohlrogge J, Pollard M. 2007. Monoacylglycerols are components of root waxes and can be produced in the aerial cuticle by ectopic expression of a suberin-associated acyltransferase. Plant physiology **144**, 1267–1277.

Li-Beisson Y, Shorrosh B, Beisson F, *et al.* 2010. Acyl-lipid metabolism. The Arabidopsis book **8**, e0133.

Liu T, Kreszies T. 2023. The exodermis: A forgotten but promising apoplastic barrier. Journal of plant physiology **290**, 154118.

Lu H-P, Gao Q, Han J-P, Guo X-H, Wang Q, Altosaar I, Barberon M, Liu J-X, Gatehouse AMR, Shu Q-Y. 2022. An ABA‐serotonin module regulates root suberization and salinity tolerance. The new phytologist **236**, 958–973.

Miyashima S, Nakajima K. 2011. The root endodermis: a hub of developmental signals and nutrient flow. Plant signaling & behavior **6**, 1954–1958.

Pireyre M, Burow M. 2015. Regulation of MYB and bHLH transcription factors: a glance at the protein level. Molecular plant **8**, 378–388.

Quiroga M, Guerrero C, Botella MA, Barceló A, Amaya I, Medina MI, Alonso FJ, de Forchetti SM, Tigier H, Valpuesta V. 2000. A tomato peroxidase involved in the synthesis of lignin and suberin. Plant physiology **122**, 1119–1127.

Rains MK, Gardiyehewa de Silva ND, Molina I. 2018. Reconstructing the suberin pathway in poplar by chemical and transcriptomic analysis of bark tissues. Tree physiology **38**, 340–361.

Ranathunge K, Lin J, Steudle E, Schreiber L. 2011. Stagnant deoxygenated growth enhances root suberization and lignifications, but differentially affects water and NaCl permeabilities in rice (Oryza sativa L.) roots. Plant, cell & environment **34**, 1223–1240.

Reynoso MA, Borowsky AT, Pauluzzi GC, *et al.* 2022. Gene regulatory networks shape developmental plasticity of root cell types under water extremes in rice. Developmental cell **57**, 1177-1192.e6.

Ritchie ME, Phipson B, Wu D, Hu Y, Law CW, Shi W, Smyth GK. 2015. limma powers differential expression analyses for RNA-sequencing and microarray studies. Nucleic acids research **43**, e47.

Robbins NE, Trontin C, Duan L, Dinneny JR. 2014. Beyond the barrier: Communication in the root through the endodermis. Plant physiology **166**, 551–559.

Ron M, Kajala K, Pauluzzi G, *et al.* 2014. Hairy root transformation using Agrobacterium rhizogenes as a tool for exploring cell type-specific gene expression and function using tomato as a model. Plant physiology **166**, 455–469.

Rushton PJ, Somssich IE, Ringler P, Shen QJ. 2010. WRKY transcription factors. Trends in plant science **15**, 247–258.

Salas-González I, Reyt G, Flis P, *et al.* 2021. Coordination between microbiota and root endodermis supports plant mineral nutrient homeostasis. Science (New York, N.Y.) **371**, eabd0695.

Serra O, Geldner N. 2022. The making of suberin. The new phytologist **235**, 848–866.

Shiono K, Yamauchi T, Yamazaki S, Mohanty B, Malik AI, Nagamura Y, Nishizawa NK, Tsutsumi N, Colmer TD, Nakazono M. 2014. Microarray analysis of laser-microdissected tissues indicates the biosynthesis of suberin in the outer part of roots during formation of a barrier to radial oxygen loss in rice (Oryza sativa). Journal of experimental botany **65**, 4795–4806.

Shukla V, Barberon M. 2021. Building and breaking of a barrier: Suberin plasticity and function in the endodermis. Current opinion in plant biology **64**, 102153.

Shukla V, Han J-P, Cléard F, *et al.* 2021. Suberin plasticity to developmental and exogenous cues is regulated by a set of MYB transcription factors. Proceedings of the National Academy of Sciences of the United States of America **118**, e2101730118.

Soler M, Serra O, Molinas M, Huguet G, Fluch S, Figueras M. 2007. A genomic approach to suberin biosynthesis and cork differentiation. Plant physiology **144**, 419–431.

Su Y, Feng T, Liu C-B, *et al.* 2023. The evolutionary innovation of root suberin lamellae contributed to the rise of seed plants. Nature plants **9**, 1968–1977.

Sun C, Yao G-F, Li L-X, Li T-T, Zhao Y-Q, Hu K-D, Zhang C, Zhang H. 2023. E3 ligase BRG3 persulfidation delays tomato ripening by reducing ubiquitination of the repressor WRKY71. Plant physiology **192**, 616–632.

To A, Joubès J, Thueux J, Kazaz S, Lepiniec L, Baud S. 2020. AtMYB92 enhances fatty acid synthesis and suberin deposition in leaves of *Nicotiana benthamiana*. The Plant journal: for cell and molecular biology **103**, 660–676.

Townsley BT, Covington MF, Ichihashi Y, Zumstein K, Sinha NR. 2015. BrAD-seq: Breath Adapter Directional sequencing: a streamlined, ultra-simple and fast library preparation protocol for strand specific mRNA library construction. Frontiers in plant science **6**, 366.

Ursache R, Andersen TG, Marhavý P, Geldner N. 2018. A protocol for combining fluorescent proteins with histological stains for diverse cell wall components. The Plant journal: for cell and molecular biology **93**, 399–412.

Ursache R, De Jesus Vieira Teixeira C, Dénervaud Tendon V, *et al.* 2021. GDSL-domain proteins have key roles in suberin polymerization and degradation. Nature plants **7**, 353–364.

Verbon EH, Liberman LM, Zhou J, Yin J, Pieterse CMJ, Benfey PN, Stringlis IA, de Jonge R. 2023. Cell-type-specific transcriptomics reveals that root hairs and endodermal barriers play important roles in beneficial plant-rhizobacterium interactions. Molecular plant **16**, 1160–1177.

Wang D, Jiang C, Liu W, Wang Y. 2020*a*. The WRKY53 transcription factor enhances stilbene synthesis and disease resistance by interacting with MYB14 and MYB15 in Chinese wild grape. Journal of experimental botany **71**, 3211–3226.

Wang Z, Liu L, Su H, Guo L, Zhang J, Li Y, Xu J, Zhang X, Guo Y-D, Zhang N. 2020*b*. Jasmonate and aluminum crosstalk in tomato: Identification and expression analysis of WRKYs and ALMTs during JA/Al-regulated root growth. Plant physiology and biochemistry **154**, 409–418.

Wang X, Niu Y, Zheng Y. 2021. Multiple functions of MYB transcription factors in abiotic stress responses. International journal of molecular sciences **22**, 6125.

Wei X, Lu W, Mao L, Han X, Wei X, Zhao X, Xia M, Xu C. 2020*a*. ABF2 and MYB transcription factors regulate feruloyl transferase FHT involved in ABA-mediated wound suberization of kiwifruit. Journal of experimental botany **71**, 305–317.

Wei X, Mao L, Wei X, Xia M, Xu C. 2020*b*. MYB41, MYB107, and MYC2 promote ABA-mediated primary fatty alcohol accumulation via activation of AchnFAR in wound suberization in kiwifruit. Horticulture research **7**.

Woolfson KN, Esfandiari M, Bernards MA. 2022. Suberin biosynthesis, assembly, and regulation. Plants **11**, 555.

Wu K-L. 2005. The WRKY family of transcription factors in rice and Arabidopsis and their origins. DNA research: an international journal for rapid publication of reports on genes and genomes **12**, 9–26.

Wu F-H, Shen S-C, Lee L-Y, Lee S-H, Chan M-T, Lin C-S. 2009. Tape-Arabidopsis Sandwich - a simpler Arabidopsis protoplast isolation method. Plant methods **5**.

Xie M, Zhang J, Tschaplinski TJ, Tuskan GA, Chen J-G, Muchero W. 2018. Regulation of lignin biosynthesis and its role in growth-defense tradeoffs. Frontiers in plant science **9**, 1427.

Xie M, Zhang J, Yao T, *et al.* 2020. Arabidopsis C-terminal binding protein ANGUSTIFOLIA modulates transcriptional co-regulation of MYB46 and WRKY33. The new phytologist **228**, 1627–1639.

Xu W, Dubos C, Lepiniec L. 2015. Transcriptional control of flavonoid biosynthesis by MYB–bHLH–WDR complexes. Trends in plant science **20**, 176–185.

Xu X, Guerriero G, Berni R, Sergeant K, Guignard C, Lenouvel A, Hausman J-F, Legay S. 2022*a*. MdMYB52 regulates lignin biosynthesis upon the suberization process in apple. Frontiers in plant science **13**.

Xu H, Liu P, Wang C, *et al.* 2022*b*. Transcriptional networks regulating suberin and lignin in endodermis link development and ABA response. Plant physiology **190**, 1165–1181.

Young MD, Wakefield MJ, Smyth GK, Oshlack A. 2010. Gene ontology analysis for RNA-seq: accounting for selection bias. Genome biology **11**, R14.

Zhang L, Merlin I, Pascal S, Bert P-F, Domergue F, Gambetta GA. 2020. Drought activates MYB41 orthologs and induces suberization of grapevine fine roots. Plant direct **4**.

Zheng Z, Qamar SA, Chen Z, Mengiste T. 2006. Arabidopsis WRKY33 transcription factor is required for resistance to necrotrophic fungal pathogens. The Plant journal: for cell and molecular biology **48**, 592–605.

Zimmermann IM, Heim MA, Weisshaar B, Uhrig JF. 2004. Comprehensive identification of *Arabidopsis thaliana* MYB transcription factors interacting with R/B‐like BHLH proteins. The Plant journal: for cell and molecular biology **40**, 22–34.

Figure & legends

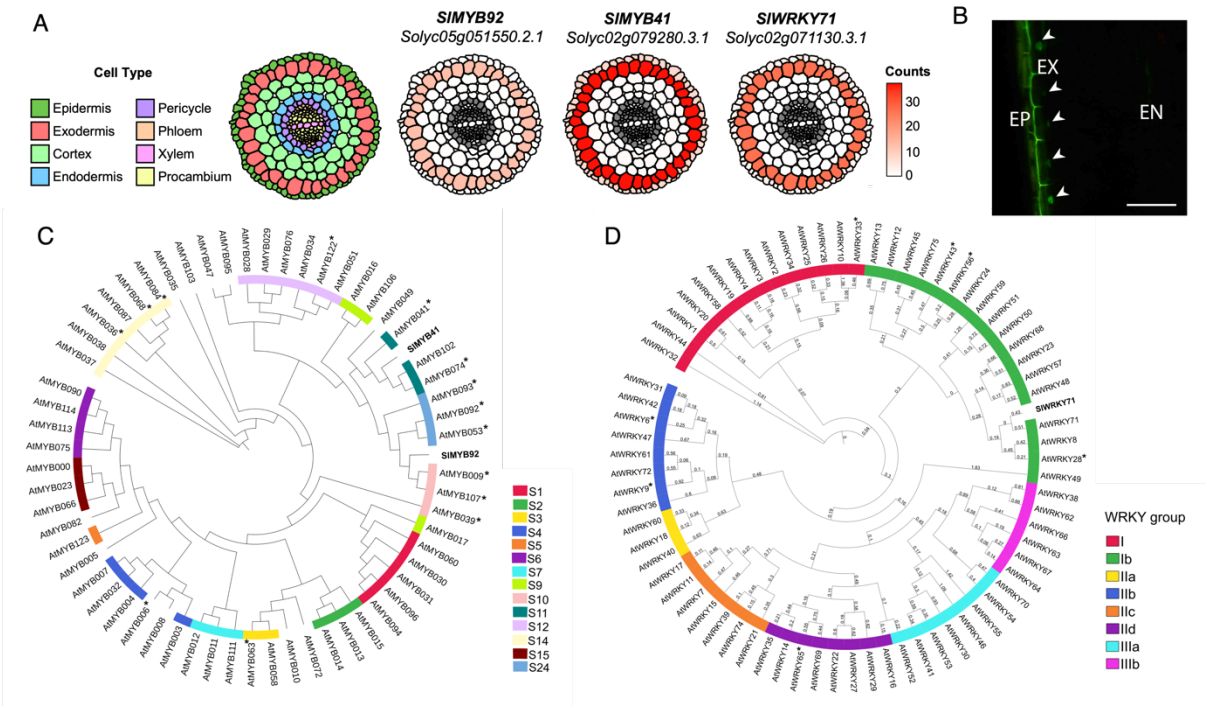

Figure 1: *SlMYB92*, *SlMYB41* and *SlWRKY71* are exodermis-enriched TFs with homologs with roles in regulating suberin.

A: Cell type-enriched gene expression heatmaps for *SlMYB92, SlMYB41* and *SlWRKY71*of translatome data from Kajala et al. (2021).

B: Transcriptional fusion *proSlMYB92:nlsGFP* drives expression in exodermis in tomato hairy root cultures. Note that autofluorescence from the exodermal and endodermal lignin are also picked up in the GFP excitation waveband. The nuclear GFP signal is indicated with arrowheads. Transcriptional fusions of *proSlMYB41 and proSlWRKY71* are previously published (Kajala *et al.*, 2021). Scale bar, 100 µm.

C-D: SlMYB41, SlMYB92 and SlWRKY71 are related to Arabidopsis MYB and WRKY TFs that regulate suberization. Representative phylogenetic trees showing the closest Arabidopsis homologs for (C) SlMYB4 and SlMYB92 and (D) SlWRKY71. The trees were inferred using the maximum likelihood method with 1000 bootstraps using iQ-TREE. Putative full length MYB and WRKY amino acid sequences were aligned with MAFFT. All MYBs and WRKYs indicated with an asterisk (*) have described functions linked with suberization. The MYB subgroups ("S") are annotated in colored boxes according to Dubos et al (2010). WRKY groups are annotated with colored boxes according to Eulgem et al. (2000) and Wu et al. (2005).

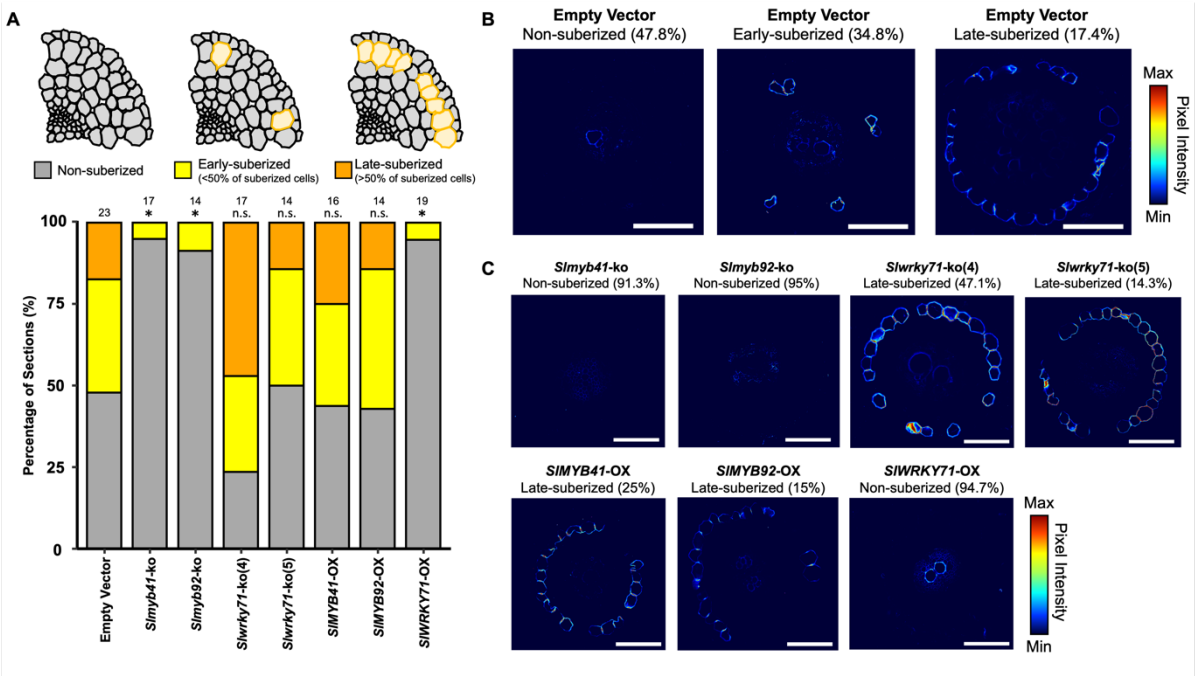

Figure 2: Perturbations on SlMYB41, SlMYB92 and SlWRKY71 expression affect the suberization of tomato exodermis.

A: Percentage of cross sections showing a non-suberized, an early-suberized (suberin in less than 50% of exodermal cells) or a late-suberized (suberin in more than 50% of exodermal cells) exodermis phenotype in hairy-root cultures of the control (empty vector), CRISPR knock-out lines (*Slmyb41*-ko, *Slmyb92*-ko, *Slwrky71*-ko(4) and *Slwrky71*-ko(5)) and overexpressing lines (*SlMYB41*-OX, *SlMYB92*-OX and *SlWRKY71*-OX). The number above the bars represents the number (n) of individual roots examined in each genotype. Asterisks denotes statistically significant differences between each line in comparison to the empty vector control, whereas n.s. indicates no significant differences ($P < 0.05$, chi-squared test).

B: Representative images of Fluorol Yellow-stained cross sections of the control hairy-root line (empty vector) showing a non-suberized, an early-suberized and a late-suberized phenotype. The percentage numbers on top of the images represent the percentage of cross-sections showing the indicated suberization phenotype. Scale bars represent 100 µm.

C: Representative images of Fluorol Yellow-stained cross sections of the knock-out and overexpressing hairy-root lines. The percentage numbers on top of the images represent the percentage of cross-sections showing the indicated suberization phenotype. Scale bars represent 100 µm.

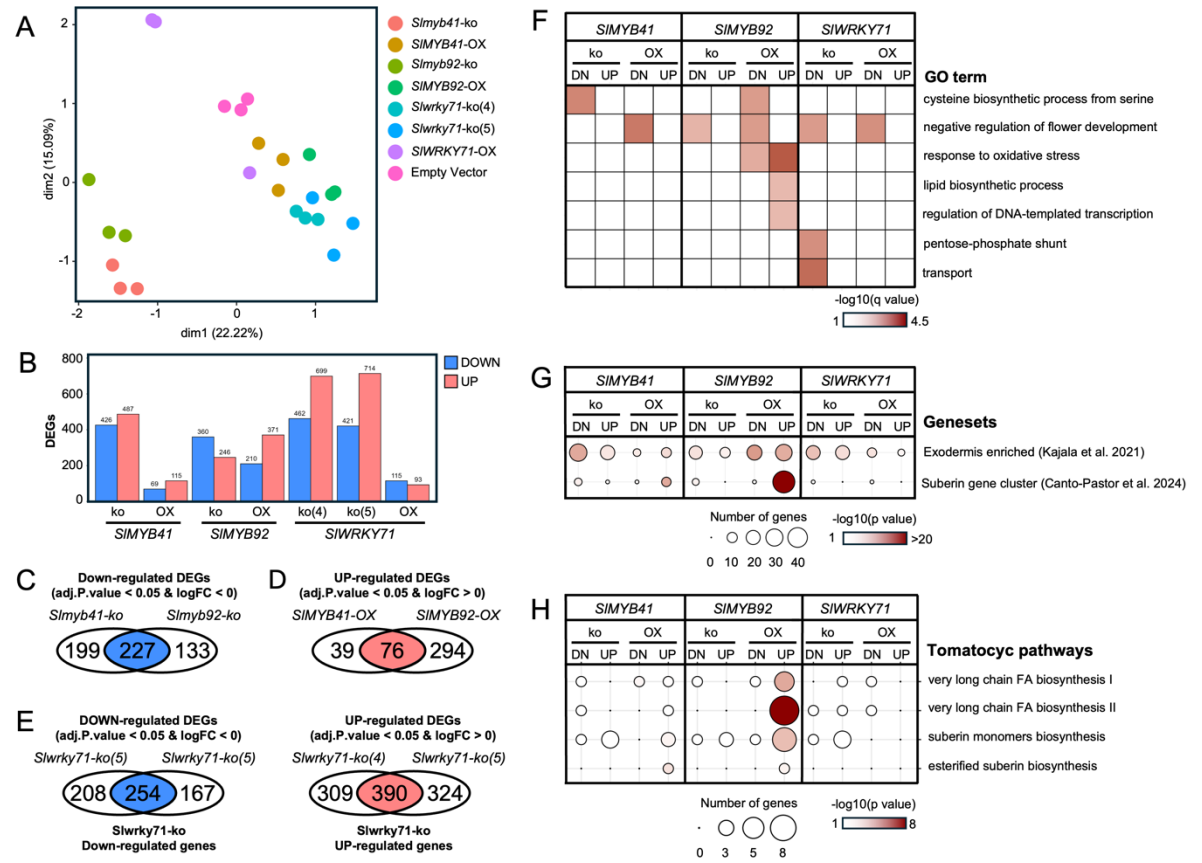

Figure 3: Transcriptome analysis of TF knockouts (kos) (*Slmyb41-ko, Slmyb92-ko, Slwrky71-*ko(4) *and Slwrky71*-ko(5)) and overexpressors (OX) (SlMYB41-OX, SlMYB92-OX and SlWRKY71-OX) in tomato hairy root cultures.

A: Multidimensional scaling (MDS) plot showing the distance between samples.

B: Number of up (FC > 0) and down (FC < 0) DEGs identified in each line with an FDR threshold of 0.05.

C: Venn diagram showing the overlap between down-regulated genes in *Slmyb41*-ko and *Slmyb92*-ko.

D: Venn diagrams showing the overlap between the up-regulated genes between *SlMYB41*-OX and *SlMYB92*-OX.

E: Venn diagrams showing the overlap between DOWN and UP regulated DEGs between *Slwrky71*-ko(4) and *Slwrky71*-ko(5). DEGs found in both independent lines were considered as down or upregulated in *Slwrky71*-ko.

F: Heatmap showing the q-value significance (-log10(q value)) of GO terms enriched in the ko and OX lists of DOWN (DN) or UP regulated list of DEGs.

G: Bubble heatmap plots showing the number of DEG genes that overlap with previously annotated list of exodermis enriched (Kajala et al. 2021) and root suberin co-expressed module (Canto-Pastor et al. 2024). Statistical significance of the overlap between datasets is indicated (hypergeometric distribution).

H: Bubble heatmap plots showing the number of DEG genes that overlap with genes annotated as involved with FA and suberin biosynthesis according to the tomatocyc database. Statistical significance of the overlap between datasets is indicated (hypergeometric distribution).

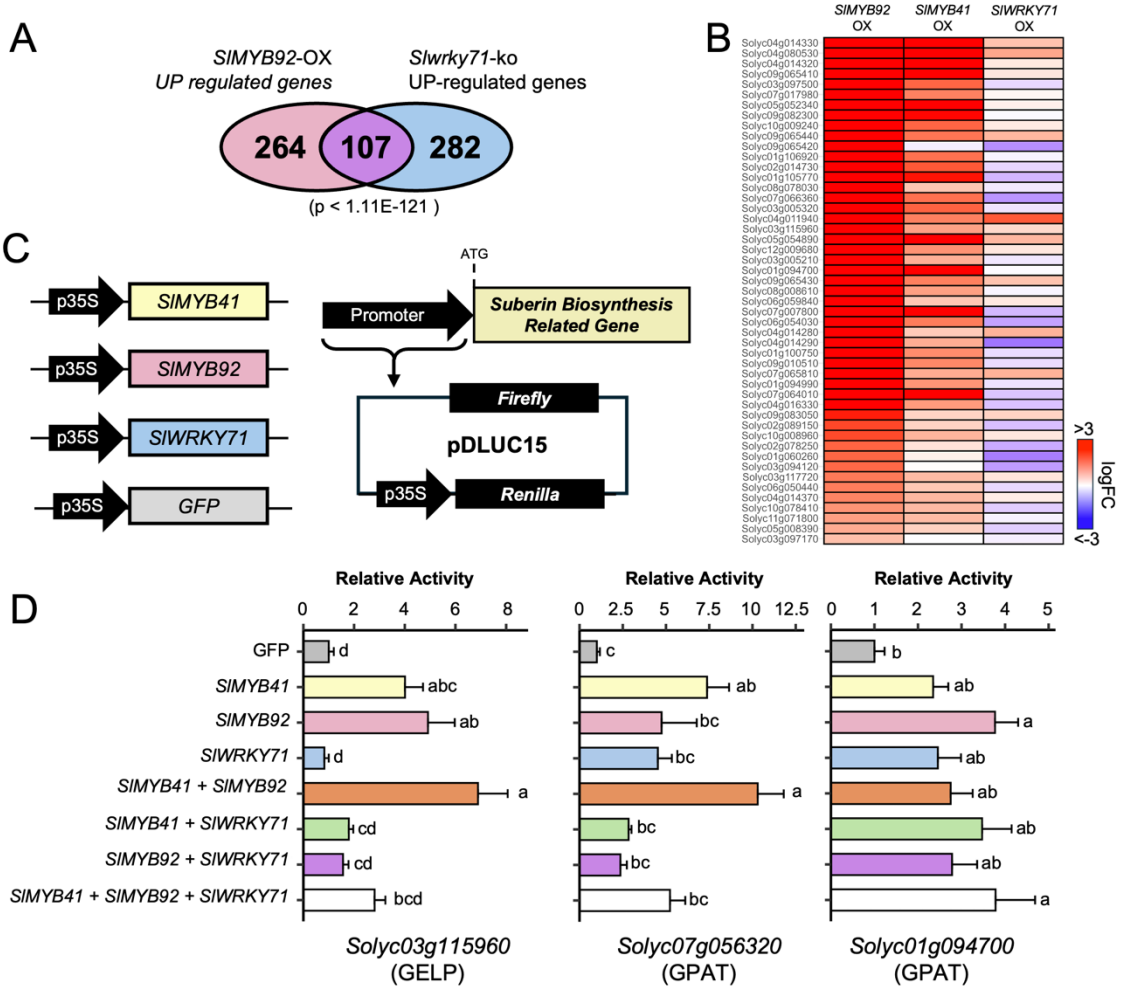

Figure 4: SlMYBs and SlWRKY71 antagonistically regulate the expression of suberin related biosynthesis genes.

A: Venn diagram showing the overlap between *SlMYB92*-OX, and *Slwrky71*-ko upregulated genes (FDR < 0.05, logFC > 0). Statistical significance of the overlap between genesets is indicated (hypergeometric distribution).

B: Heatmap showing the logFC values of genes in the *SlMYB92*-OX, *SlMYB41*-OX and *SlWRKY71*-OX. Values are presented for the genes that are significantly up-regulated in the *SlMYB92-OX* and annotated in the suberin co-expression cluster (Canto-Pastor et al. 2024).

C: Schematic diagrams of constructs used for the transactivation assays.

D: Transactivation assays in protoplasts of *A. thaliana*. The protoplasts were co-transformed with the pDLUC15 vector expressing the Firefly luciferase under the control of the promoter of interest and with different combinations of overexpressed transcription factors, as indicated in the X-axis. The pDLUC15 contained also the *35S::Renilla* luciferase, used as internal control. The Firefly to Renilla luciferase activity ratios were normalized to the average ratios of the GFP samples. Data represent mean ± SE (n = 4-5). Different letters indicate statistically significant differences (1-way ANOVA followed by a post-hoc Tukey test, p < 0.05).

```
CLUSTAL 2.1 multiple sequence alignment


Slwrky71_ko_#4                  ------------MGDELRDLYYHQPFQEDIKHDSSMVQNIHMLDPTFMSY
Slwrky71_ko_#5                  ------------MGDELRDLYYHQPFQEDIKHDSSMVQNIHMLDPTFMSY
ITAG2.4|Solyc02g071130.2.1      ------------MGDELRDLYYHQPFQEDIKHDSSMVQNIHMLDPTFMSY
ITAG4.0|Solyc02g071130.4.1      PFLSSFYFLFFNMGDELRDLYYHQPFQEDIKHDSSMVQNIHMLDPTFMSY
ITAG3.2|Solyc02g071130.3.1      ------------------------------------------------
AT1G29860.1                     ------------MDDHVEHNYNTSLEEVHFKSLSDCLQSSLVMDYNSLEK


Slwrky71_ko_#4                  TSEYLHGSSSDYITNNSLGKPFGFSTLSSLKDDDIMKQDHVDANVNYINN
Slwrky71_ko_#5                  TSEYLHGSSSDYITNNSLGKPFGFSTLSSLKDDDIMKQDHVDANVNYINN
ITAG2.4|Solyc02g071130.2.1      TSEYLHGSSSDYITNNSLGKPFGFSTLSSLKDDDIMKQDHVDANVNYINN
ITAG4.0|Solyc02g071130.4.1      TSEYLHGSSSDYITNNSLGKPFGFSTLSSLKDDDIMKQDHVDANVNYINN
ITAG3.2|Solyc02g071130.3.1      ------------------------------------------------
AT1G29860.1                     VFKFSPYSSPFQSVSPSVNNPYLN-----------------------LTS


Slwrky71_ko_#4                  NNDVVGGSETPVTPNSSISNSSSNGDHEDSNKKDKQVKDETLEDGEDASK
Slwrky71_ko_#5                  NNDVVGGSETPVTPNSSISNSSSNGDHEDSNKKDKQVKDETLEDGEDASK
ITAG2.4|Solyc02g071130.2.1      NNDVVGGSETPVTPNSSISNSSSNGDHEDSNKKDKQVKDETLEDGEDASK
ITAG4.0|Solyc02g071130.4.1      NNDVVGGSETPVTPNSSISNSSSNGDHEDSNKKDKQVKDETLEDGEDASK
ITAG3.2|Solyc02g071130.3.1      ------------------------------------------------
AT1G29860.1                     NSPVVSSSSNEGEPKENTNDKSDQMEDNEGDLHG---------VGESSKQ


Slwrky71_ko_#4                  KESKAKKKGEKKQRPPKFAFMTKSEVDHLEDGYRWRKYGQKAVKNSPYPR
Slwrky71_ko_#5                  KESKAKKKGEKKQRPPKFAFMTKSEVDHLEDGYRWRKYGQKAVKNSPYPR
ITAG2.4|Solyc02g071130.2.1      KESKAKKKGEKKQRPPKFAFMTKSEVDHLEDGYRWRKYGQKAVKNSPYPR
ITAG4.0|Solyc02g071130.4.1      KESKAKKKGEKKQRPPKFAFMTKSEVDHLEDGYRWRKYGQKAVKNSPYPR
ITAG3.2|Solyc02g071130.3.1      --------------------MTKSEVDHLEDGYRWRKYGQKAVKNSPYPR
AT1G29860.1                     LTKQGKKKGEKKEREVRVAFMTKSEIDHLEDGYRWRKYGQKAVKNSPYPR
                                                     *****:************************

Slwrky71_ko_#4                  SYYRCTSQKCQVKKRVERSYQDPSIVITTYEGQHNHHH------------
Slwrky71_ko_#5                  SYYRCTSQKCQVKKRVERSYQDPSIVITTYEGQHNHHLPATLH-------
ITAG2.4|Solyc02g071130.2.1      SYYRCTSQKCQVKKRVERSYQDPSIVITTYEGQHNHHLPATLRGSVARML
ITAG4.0|Solyc02g071130.4.1      SYYRCTSQKCQVKKRVERSYQDPSIVITTYEGQHNHHLPATLRGSVARML
ITAG3.2|Solyc02g071130.3.1      SYYRCTSQKCQVKKRVERSYQDPSIVITTYEGQHNHHLPATLRGSVARML
AT1G29860.1                     SYYRCTTQKCNVKKRVERSFQDPSIVITTYEGKHNHPIPSTLRGTVAAEH
                                ******:***:********:************:***

Slwrky71_ko_#4                  ------------------------------------------------
Slwrky71_ko_#5                  ------------------------------------------------
ITAG2.4|Solyc02g071130.2.1      NPSMLAQPSPLMAPQASFHQEFIMSQMPQFYGHANVFANSSMYHQNLNHH
ITAG4.0|Solyc02g071130.4.1      NPSMLAQPSPLMAPQASFHQEFIMSQMPQFYGHANVFANSSMYHQNLNHH
ITAG3.2|Solyc02g071130.3.1      NPSMLAQPSPLMAPQASFHQEFIMSQMPQFYGHANVFANSSMYHQNLNHH
AT1G29860.1                     LLVHRGGGGSLLHSFPRHHQDFLMMKHSPAN--YQSVGSLSYEHGHGTSS


Slwrky71_ko_#4                  ------------------------------
Slwrky71_ko_#5                  ------------------------------
ITAG2.4|Solyc02g071130.2.1      QQMQLPHPHHDYGLLQDMVPSMFNLKQEP
ITAG4.0|Solyc02g071130.4.1      QQMQLPHPHHDYGLLQDMVPSMFNLKQEP
ITAG3.2|Solyc02g071130.3.1      QQMQLPHPHHDYGLLQDMVPSMFNLKQEP
AT1G29860.1                     YNFNNNQPVVDYGLLQDIVPSMFSKNES-…
```

Figure S1: SlWRKY71 sequences and truncations generated with gene editing. Multiple sequence alignment made using ClustalW. Three different versions of SlWRKY71 from three tomato genome annotations (ITAG2.4, ITAG3.2 and ITAG4.0) were obtained from Phytozome, while the one corresponding to *A. thaliana* AT1G29860.1 was obtained from TAIR Araport 11. The protein sequences of *Slwrky71*-ko(4) and *Slwrky71*-ko(5) lines were extrapolated based on the sequencing results of the genomic fragment.

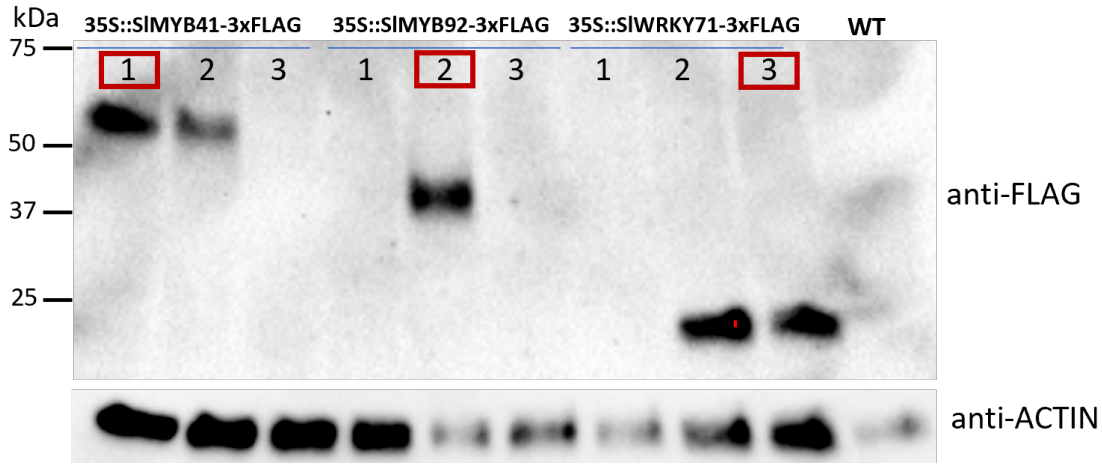

Figure S2: TF overexpression is detected on protein level. Western blot experiment using total protein lysates of hairy roots. Three independent transgenic lines were used to verify the presence of the overexpressed proteins with the use of the anti-FLAG antibody. The anti-ACTIN antibody was instead used to verify the correct loading of the samples. One line for each construct (circled in red) was selected for further experiments.

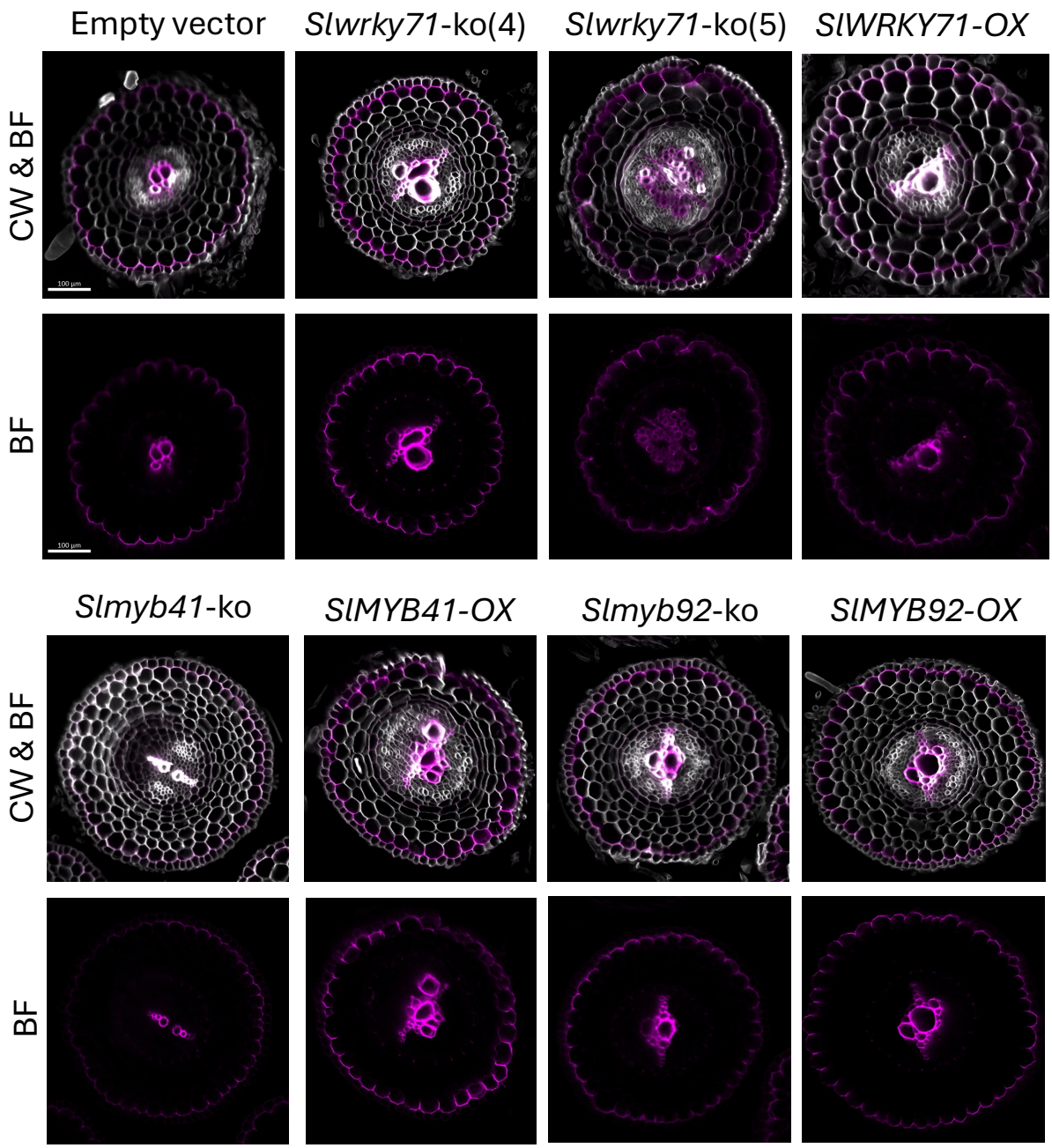

Figure S3: Exodermal lignin is unaffected by *SlMYB92*, *SlMYB41* and *SlWRKY71* perturbations. Representative images of root cross sections stained with Basic Fuchsin (BF, represented in magenta) and Calcofluor White (CW, represented in white). Lignin in the exodermal cell file remains unaffected for each genotype. Scale bars represent 100 µm.

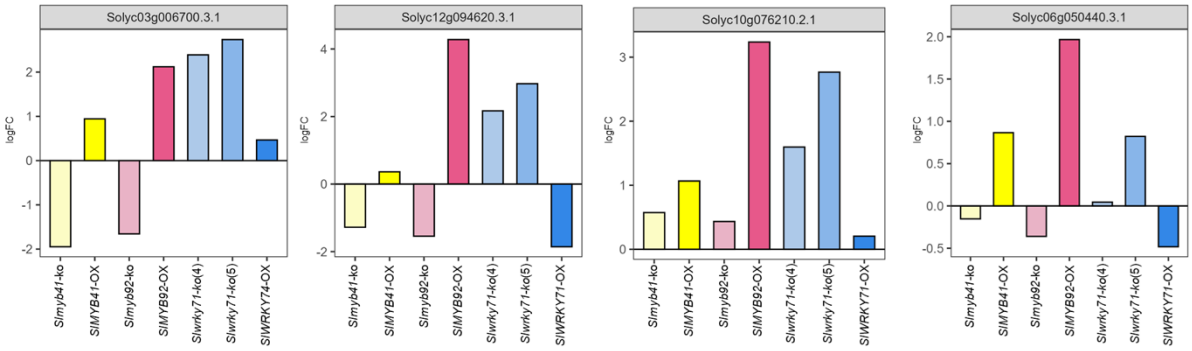

Figure S4: Expression of peroxidases and catalases is affected in TF knock outs and overexpressors. logFC of peroxidases and catalases in *Slmyb41*-ko, *SlMYB41*-OX, *Slmyb92*-ko, *SlMYB92*-OX, *Slwrky71*-ko(4), *Slwrky71*-ko(5) and SlWRKY71-OX in comparison to WT hairy-roots.

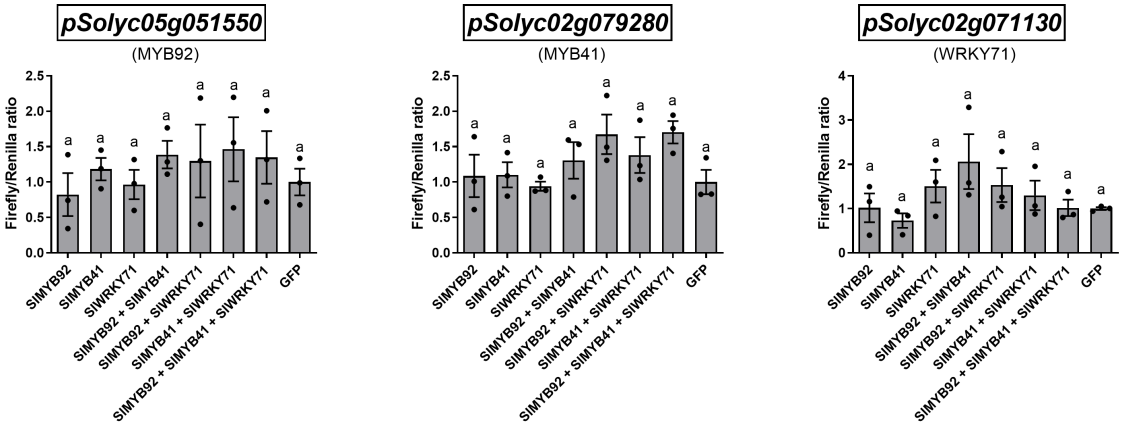

Figure S5: Transactivation assays of *SlMYB92*, *SlMYB41* and *SlWRKY71* promoters in protoplasts of *A. thaliana*. The protoplasts were co-transformed with the pDLUC15 vector expressing the firefly luciferase under the control of the promoter of interest and with different combinations of overexpressed transcription factors, as indicated in the X axis. The pDLUC15 contained also the *35S::Renilla* luciferase, used as internal control. Instead, when the transactivation of *pSolyc02g071130* in the vector pGWL7 was investigated, the samples were also transfected with a separate vector containing the *35S::Renilla* luciferase. The Firefly to Renilla luciferase activity ratios were normalized to the average ratios of the GFP samples. Data represents mean ± SE, each dot represents a biological replicate (n = 3). Different letters indicate statistically significant differences (1-way ANOVA followed by a post-hoc Tukey test, $p < 0.05$).